



Review

Diverse Methods to Nanomanufacture Colloidal Dispersions of Polyaniline without Templates

Cesar A. Barbero

Research Institute for Energy Technologies and Advanced Materials (IITEMA), National University of Río Cuarto (UNRC)-National Council of Scientific and Technical Research (CONICET), Río Cuarto 5800, Argentina; cesarbarbero@gmail.com

Abstract: Different methods which could be used to produce colloidal dispersions of polyaniline (PANI) nano-objects without templates are described. While the methods are non-deterministic, different nano-objects (nanospheres, nanofibers, nanobelts, nanorice, nanotubes, nanorods, nanodisks, etc.) can be produced. Those most used are: (i) solution polymerization with steric stabilizers (SPS) to produce nanospheres, (ii) interfacial polymerization (IP) to produce nanofibers and (iii) solution polymerization in the presence of additives (SPA) to produce nanotubes. Oxidation of aniline in aqueous solution could produce nanotubes, nanofibers and other shapes by controlling mass transport/concentration of reactants, pH, and the presence of oligomers/additives. The different models proposed to explain the formation of various nano-objects are discussed. Mechanochemical polymerization (MCP) could produce nanofibers or nanospheres by controlling the aniline/oxidant ratio. PANI nanospheres of tunable sizes can also be produced by nanoprecipitation (NPT) of preformed PANI from its solutions using an antisolvent. The geometrical constraints to the small nano-objects made of high-molecular-weight rigid polymers are described. The conditions to produce nanostructures also affect the intrinsic properties of PANI (conductivity, crystallinity, and electroactivity). Selected technological applications of PANI nano-objects manufactured as colloidal dispersions without templates are discussed. Based on the reviewed work and models, future lines of work are proposed.



Citation: Barbero, C.A. Diverse Methods to Nanomanufacture Colloidal Dispersions of Polyaniline without Templates. *Nanomanufacturing* **2023**, *3*, 57–90. <https://doi.org/10.3390/nanomanufacturing3010005>

Academic Editor:
Andres Castellanos-Gomez

Received: 30 December 2022
Revised: 15 January 2023
Accepted: 31 January 2023
Published: 7 February 2023



Copyright: © 2023 by the author. Licensee MDPI, Basel, Switzerland. This article is an open access article distributed under the terms and conditions of the Creative Commons Attribution (CC BY) license (<https://creativecommons.org/licenses/by/4.0/>).

Keywords: template free; polyaniline; nano-objects; colloids; synthesis

1. Introduction

Polyaniline (PANI) is the most widely studied and technologically used conducting polymer [1]. The history of conducting polymers began with the publication by Shirakawa et al. (1979), describing the huge increase in conductivity upon p-doping with the halogen of polyacetylene [2]. However, the products of aniline oxidation (so called “aniline blacks”) were discovered by Runge in 1834 [3]. That PANI was a conductive polymer, electroactive and could be doped by protons was known in the 1960s [4]. Its role as a conducting polymer was rediscovered by MacDiarmid in the 1980s [5]. Unlike polyacetylene, aniline can be polymerized by oxidation in aqueous solution without catalysts and the resulting polymer is much more stable in air [6]. However, similar to other conducting polymers, it is insoluble in most common solvents and does not show T_g or T_m below decomposition. To use PANI in technological applications (anticorrosive coatings, electronic thin films, electrochromics, conductive ink, etc.), the polymer has to be processible. While thin films can be produced by in situ polymerization [7], the polymerization mixture is quite corrosive and only thin (<300 nm) films can be produced. With the advent of nanotechnology, a solution is at hand in the form of a colloidal solution of conducting nanoparticles. In addition to the technological applications as films, nanoparticles could be used for a variety of applications: to form multilayers, porous films for sensors, for photothermal therapy and even to produce N-doped carbon nanoparticles [8]. The published work on

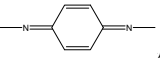
polyaniline nanoparticles exceeds 4000 results. However, the vast majority involves the formation of mixed nanoparticles or nanocomposites together with metals [9], oxides [10], polymers [11], or nanocarbons [12]. Since the properties of those composite nanoparticles and nanocomposites depend on both components, this review only deals with the synthesis, characterization and applications of colloidal dispersions of PANI nanoparticles. One clear implication is that the large body of work on electrochemical polymerization of anilines will not be discussed [13]. Moreover, some widely used methods to manufacture PANI nanoparticles involves using porous hard membranes (e.g., alumina membranes) [14], or organized systems (e.g., micelles) as templates [15]. Those methods require a removal step for the template and, in principle, are deterministic in the sense that the shape/size of the nano-object is determined directly by the template.

On the other hand, the synthesis of nanotechnological species is dominated by self-formed non-deterministic systems, being metallic [16], silica [17] or polymeric [18] nanoparticles. Analogously, carbon nanotubes [19], graphene [20], and graphene-like materials [21] are made by non-deterministic processes. A similar set of methods, without templates have been shown to be effective [22], and even industrially useful [23] to produce PANI colloidal dispersions. Therefore, the published work on the nanomanufacturing of PANI as colloidal dispersions is analyzed in terms of the proposed mechanism of synthesis.

The main goal of the manufacturing of PANI nanomaterials is their use in technological applications. Since PANI is not soluble in water or common organic solvents, the manufacturing of colloidal dispersions enables producing a PANI conductive “ink” which can be used directly or as a way to form other structures, such as films. The electronic conductivity of PANI allows the manufacturing of electrochemical sensors, anticorrosion coatings, optoelectronic films, etc. The synergy of PANI conductivity with the large surface area of PANI nano-objects allows building double-layer supercapacitors where the intrinsic electroactivity of PANI adds a pseudocapacitance contribution. Moreover, the chemical nature of PANI gives a rich surface chemistry which could be used in adsorption of charged species. The technological applications of PANI nano-objects, produced as colloidal dispersions by template-free methods, will be summarily described. The advantages observed on the use of PANI in those applications will be discussed.

2. Template-Free Synthesis of PANI as Colloidal Dispersions

The oxidative polymerization of aniline begins in solution, but the growing chain becomes insoluble and precipitates by aggregation with other chains [24]. The formation of nanoparticle dispersion involves the formation of the solid form and the stabilization against aggregation. In metallic nanoparticles, the reduction of metal ions form the nuclei which grows and some molecules, which have stabilizing moieties such as charged groups or solvophilic polymer chains, adsorb on the formed nanoparticle, stabilizing it against aggregation. The usual shape obtained is granules that are more or less spherical. Since they are crystalline, rods with different aspect ratios (length/diameter) could be obtained by using additives which adsorb on some crystalline planes. The method can be used further to form very complex and useful shapes [25]. The size depends on the number of atoms and could be of a few nanometers for metal clusters [26]. Vinyl polymers have free rotation at the C-C bonds, allowing changes in conformations to form globules in the solid state which could be quite compact. The size of the globule does not depend directly on the size of the monomer unit [27].

On the other hand, if PANI chains are rigid, due to the extended conjugation of the quinonimine units , the aggregation of different chains should produce flat ribbons, the minimum of which size is the length of the chain. Therefore, from purely geometrical analysis, it is possible to calculate a minimum size of nanospheres of PANI or length of nanofibers. The molecular mechanics (MM2 [28]), package of Chem3D Ultra 8.0[®] was used to minimize the geometry of a fully oxidized PANI (pernigraniline base, PN) showing a flat chain of conjugated quinonimine units (Figure 1A). From the oligomer with

16 rings, a mean size of the quinonimine unit of 0.75 nm is calculated. Using the reported mean degree of polymerization of PN [29], of 380 units, a minimum size of ca. 288 nm is calculated. The result is relevant since PANI chains grow in the PN state [29]. Therefore, the nanoparticles manufactured by oxidative polymerization should have mean sizes in that order or larger.

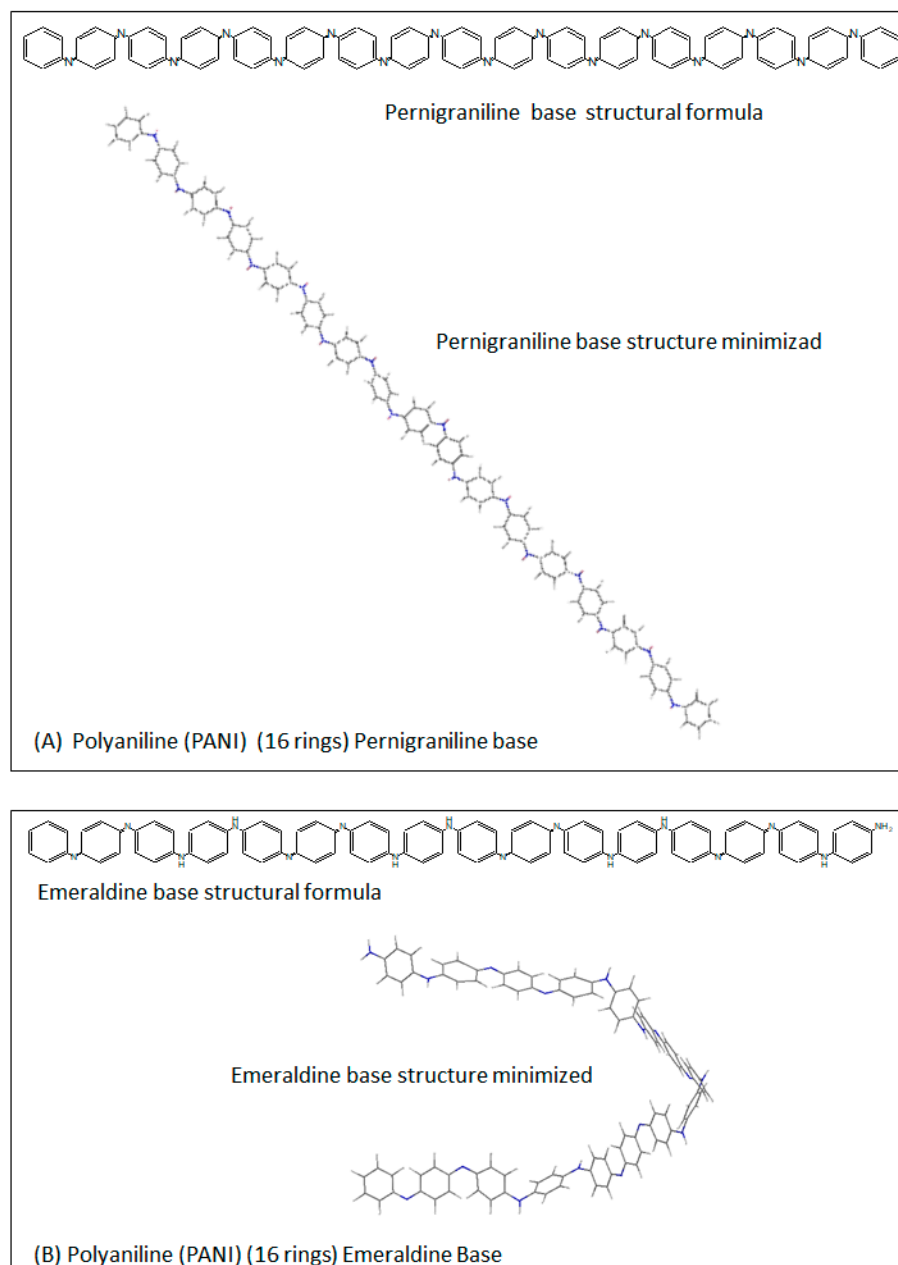
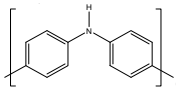


Figure 1. (A) Minimized (MM2) geometries of PANI oligomers (16 rings). (A) Pernigraniline base; (B) emeraldine base.

On the other hand, polyaniline show a large polydispersity ($\delta = 2.18$ [30]). Therefore, short chains could form small nanoparticles. Moreover, the polymerization chains terminate when the oxidant is consumed [29]. Therefore, in conditions of low local oxidant concentration, shorter chains will predominate.

Such constraints are valid for nanoparticles made of PANI (PN), with a rigid chain of planar geometry (Figure 1A). The minimization of PANI (EB) (16 rings) shows a circle-

like form due to the angle  of the secondary amine (diphenylamine) units (Figure 1B). The diameter of the circle is as low as 96 nm, allowing for small nanoparticles, or small-diameter nanotubes, to be formed.

In a first view, these smaller nanoparticles could be formed only in the manufacturing procedure where PANI (EB) aggregates to form the nanoparticles. This is true for the nanoprecipitation (Section 2.1.3). However, while PANI chains grow as PN, it is converted into EB in the termination step. Therefore, the NP could grow in an expanded linear form (PN) and then contract to the ring-like form (EB) form by the termination reaction.

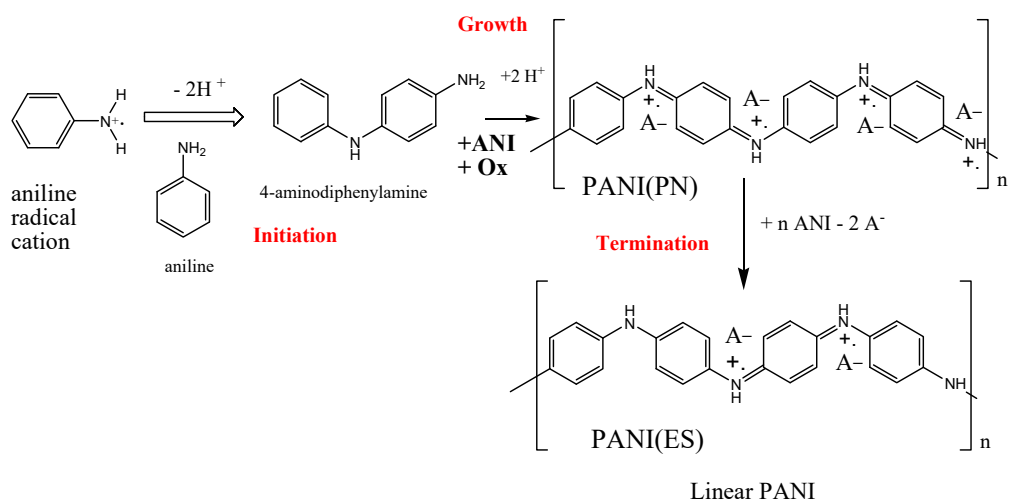
2.1. Manufacturing Colloidal Dispersions of PANI Nano-Objects by Polymerization without Templates

Aniline polymerization can be made by a variety of methods, including plasma oxidation and mechanochemistry. However, the most commonly used is so called “solution” polymerization [31]. In fact, while the polymerization begins by mixing a solution of anilinium ion with another of an oxidant, the chain becomes insoluble and particles are formed. In the absence of special conditions, a solid precipitates. Another way involves interfacial polymerization. In this method, the reaction and chain growth occurs at the interface between two immiscible solvents, being a flat interface or an emulsion of one solvent dispersed in other. Finally, a method known to produce nanoparticles is the mechanochemical (solvent-free) polymerization. Since the reactants are solid, the produced nanoparticles are not made as a dispersion but can be dispersed in a solvent (e.g., water) during washing.

2.1.1. Solution Polymerization (SP)

Polymerization of aniline is made by mixing a solution of aniline salt with a solution of an oxidant [31]. After the reaction is finished, the polymer is filtered out of the solution.

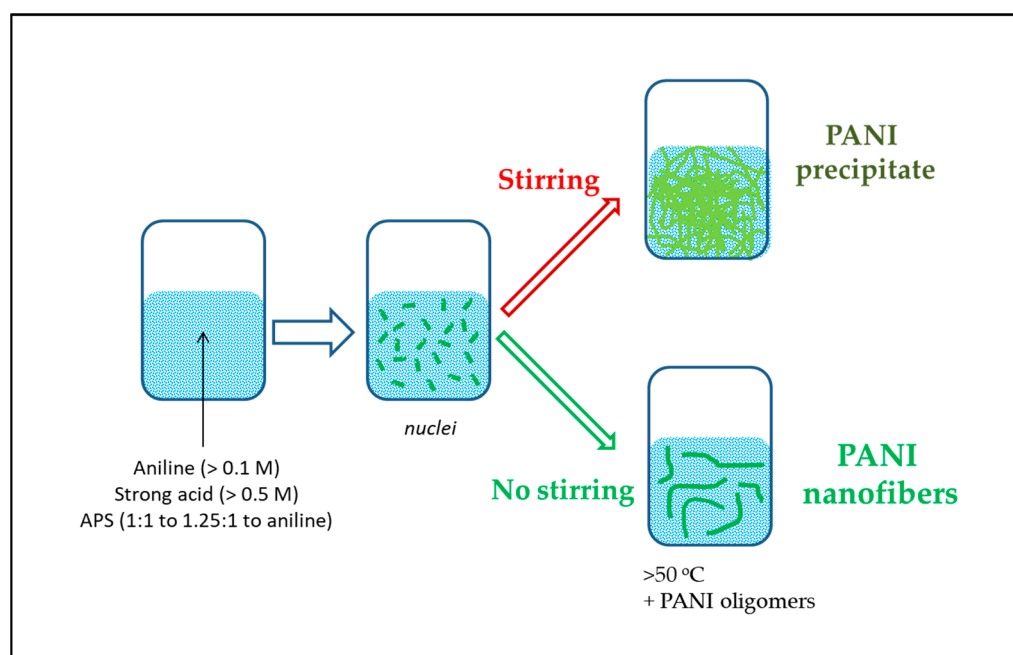
The polymerization mechanism is shown in Scheme 1. As can be seen, the polymer grows in the pernigraniline (PN, fully oxidized form) by addition of aniline molecules at the extreme of the chain [32].



Scheme 1. Mechanism of aniline polymerization to produce linear PANI.

However, changing the polymerization parameters, defined nanostructures can be produced. Kaner and coworkers found the formation of PANI nanofiber dispersions by controlling the mixing of the reactants and stirring of the solution [33] (Scheme 2). Then, they extensively studied the mechanism of nanofiber formation [34–37]. The authors propose a general model of nucleation and growth of nanofibers, which occurs during any aniline polymerization. Since they assume that mass transfer is critical to the formation of

nanostructures, the reaction model will be called Mass Transport Determining Polymerization (MTDP). The nuclei are formed homogenously by the oxidation of aniline. From the nuclei, chain growth produces nanofibers. Then, new chains are formed from the nanofibers, making large PANI aggregates. If the solution is stirred, the aggregation is favored and a macroscopic precipitate is produced. Nanofiber dispersions can be readily obtained by rapidly mixing aniline, in an aqueous acidic solution, with an oxidant at higher temperatures ($>25\text{ }^{\circ}\text{C}$) and in the absence of mechanical agitation. The kind of counterion influences the size of the nanofibers. While growth in HCl gives a small diameter (ca. 30 nm), using CSA produces a larger diameter (ca. 50 nm), and HClO_4 renders the largest sizes ($>120\text{ nm}$ in diameter). Since through fast growth of chains and/or the presence of a lot of nuclei, a large number of independent fibers grow, the fibers stay dispersed in the solution and no precipitate is formed. The best conditions are: relatively high temperatures ($>50\text{ }^{\circ}\text{C}$), no agitation of the solution and addition of nucleation, forming molecules [38].

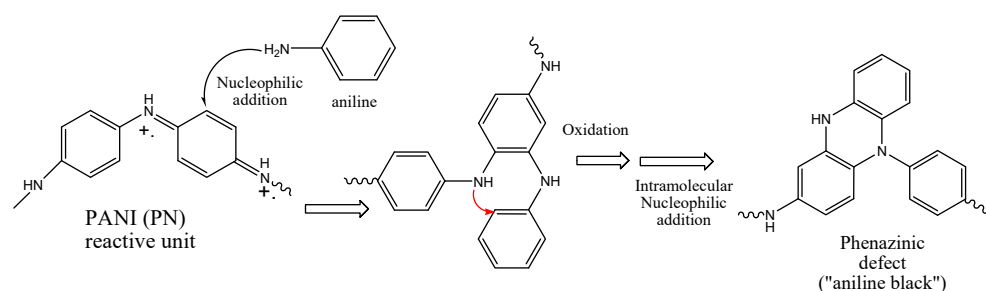


Scheme 2. Reaction scheme underlying the Mass Transport Determining Polymerization (MTDP) model.

It is known [39] that the presence of some molecules (e.g., p-phenylenediamine) affects the size and crosslinking of the fibers which constitute the PANI precipitate. Therefore, addition to the solution promotes nucleation and nanofiber formation. The method is useful in the case of PANI, but it is essential for the polymerization of substituted anilines [40]. In addition to the mechanism of nanofiber formation remains the question of dispersion stability against aggregation in water without stabilizers. In the work of Kaner and coworkers, acid (1 M) solution is used and the nanofibers are protonated not only in the imine nitrogen but also in the secondary amine groups. Therefore, the polymer has positive net charges and an electrical double layer made mainly of the mobile counterions. The repulsion of charged double layers could account for the stability of the nanofiber dispersions. In fact, increasing the pH to 5–7 induces aggregation, often irreversibly. On the other hand, the nanofiber dispersion could be purified/concentrated by centrifugation and the loose precipitate dispersed by ultrasound. Kaner and coworkers use the nucleation and growth model to explain the results assuming that all chains are linear (no ramification) and other parameters (oxidant/monomer ratio, kind and concentration of acid, etc.) have little effect. However, various groups obtain different nano-objects by polymerization of aniline in quite similar conditions, suggesting that other effects have some influence. The products are micrometric nanofibers (diameter $< 100\text{ nm}$). It should be noted that the

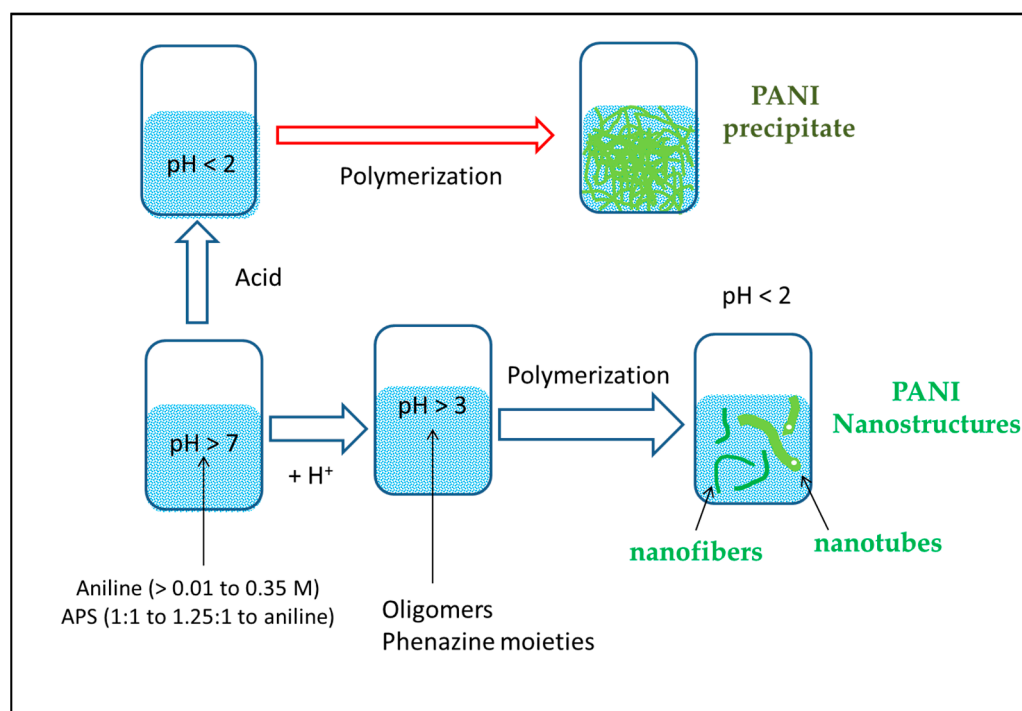
nanofibers are not compact cylinders but have a ribbon-like shape and are not straight but contain several kinks. Li et al. synthesize PANI “nanosticks” by oxidation of ANIHCl with APS [41]. The microscopic images of the nanosticks resemble Kaner’s nanofibers albeit shorter. The authors claim that ANIHCl form rod-like micelles, with neutral aniline inside, and direct the formation of the polymer as rods. They have no experimental proof of the existence of such micelles which have not been observed in the hundreds of studies of aniline polymerization. Moreover, they disregard the fact that polymerization with APS produces sulfuric acid and attribute the low conductivity of nanosticks produced in water to low doping.

Stejskal and coworkers extensively studied the polymerization of aniline and the formation of nano-objects in the absence of templates [42–49]. They obtained nanotubes, nanospheres and other shapes. The main difference with the work of Kaner and coworkers is the use of different pH values (from ca. 0 to 10–11) and changing the dopant acid. They recognize, which is unfortunately not common in the field, that oxidation with APS produces sulfuric acid, made by sulfate anions produced by persulfate reduction and protons from the electrophilic aromatic substitution in the aniline ring. Therefore, unless the solution is buffered, with a large buffer capacity, the pH will become acidic when the conversion increases. If a weak acid (e.g., acetic) is used to acidify the initial solution, the weak acid will become protonated and it will not act as a dopant of the produced PANI. Instead, the sulfate (and bisulfate) ions will remain as counterion of PANI(ES). Moreover, the fact that aniline is oxidized at neutral (or basic) pH at the beginning of the reaction gives rise to oligomers which are not linear head-to-tail para linked chains but also contain *ortho* linkages and/or phenazinic rings (Scheme 3).



Scheme 3. Mechanism of *ortho* addition of aniline to PANI (PN form) and formation of phenazinic rings. Only half of the pernigraniline tetramer unit is shown for simplicity.

The extended conjugation of linear PANI will be broken and the conductivity decreased. Moreover, packing of chains flat on each other (PN form) will not be possible. The oligomers are soluble in the solution and can self-assemble by π – π interactions and hydrogen bonding, creating insoluble solids which could template the assembly of more complex structures such as nanotubes. Therefore, two exothermic phases of nano-object formation are present: (i) formation of oligomers at high pH; (ii) PANI growth at low pH. The latter phase leads to large aggregates. Since the pH and the temperature can be continuously monitored, the reaction could be stopped at any point and the nano-objects isolated. The detailed study by Stejskal et al. has more evidence of the chemical structures, oligomers, etc., than other studies (Scheme 4) [42]. Other authors have supported the mechanism. Luo et al. polymerized different substituted anilines and found an even higher amount of phenazinic units [50]. At the same time, they were able to produce different nano-objects from those anilines.



Scheme 4. Reaction steps underlying the pH-Dependent Polymerization (pHDP) model.

The most interesting new nano-object obtained by Stejskal and coworkers are PANI open nanotubes. Since the key factor is the evolution of the pH of the solution, the model will be called pH-Dependent Polymerization (pHDP). Feng et al. observe the self-assembly of PANI oligomers and its effect on the formation of polymer nanostructures [51]. In that way, their results support the pHDP. Stejskal and coworkers used unbuffered solutions which become increasingly acidic during polymerization. Laslau et al. used a pH stat to maintain constant pH values (1, 2, 3, 4, 5 and 6) without adding different ions (buffer) which could affect the polymerization [52]. They partially confirmed and extended the pHDP model. While PANI nanotubes are formed at a constant acidity, the morphology changes with time even at constant pH. More different structures are observed, including spheres, flakes and ribbons at pH = 6, fibers and tubes at pH = 3–5, and large grains at pH < 2. Conducting nano-objects are produced at pH 1–3 while insulating structures are made at pH > 4. Interestingly, no effect of stirring was observed at any pH. The increase in pH produced decreased protonation, and increased ortho coupling, phenazine content, and sulfonation [53]. MacDiarmid and coworkers give a name to the phenazinic (Scheme 3)-containing polymers: azanes [54]. They investigated the properties of the materials and found that they have low conductivity but could form different shaped nano-objects [55]. In fact, the structures have been known for a long time since they likely constitute the “ungreeneable aniline blacks” fabricated in the 19th century [56]. The “ungreeneable” adjective implies that they could not be reduced, unlike emeraldine or nigraniline which can be reduced to green polymers [57]. Aniline black is still a commercial dye produced by oxidation of aniline, whose structure contains several phenazine units [58]. The molecule cannot be reduced nor is it conductive. Li et al. make an excellent review on the state of knowledge on the formation of PANI structures in aqueous solution [59].

The MTDP model requires controlling the stirring to produce PANI nanofibers while the pHDP requires a high initial pH to produce the oligomers which induce the formation of nanotubes. In both cases, after formation of the nanostructures, some repulsive interaction should exist (e.g., double-layer formation by protonation) to stabilize the dispersions. Otherwise, large PANI aggregates are produced. However, McDiarmid and coworkers found that it is not the synthesis processes responsible for the aggregation but the separation/purification [60]. Using conventional filtration promotes aggregation while

purifying by dialysis allows maintaining nanofiber dispersion. Another factor which has to be taken into account is that Manohar and coworkers detect the formation of micelles between aniline and persulfate ions, during the induction time of polymerization. They claimed that such micelles induce the formation of nanostructures [61]. Neelgund and Oki, polymerize aniline with APS (1:1 ratio) at 0–5 °C and a higher concentration (0.35 M) than other work, without adding acids [62]. They obtained nanospheres of 8 ± 3 nm. It is noteworthy that aniline solubility in pure water is 0.353 M at 8.6 °C [63]. In a solution which also contains 0.35 M salt (APS) and at 0–5 °C, the solubility is likely lower and spherical droplets of aniline should be present. Obviously, as the polymerization proceeds, the aniline concentration decreases and pH decreases, making the aniline protonated and soluble. In that way, the droplets dissolve. However, initially, a thin film of PANI could be formed around each droplet, creating the nanospheres. Ayad et al. polymerize aniline in water (0.07 M) by oxidation with APS, under stirring at 0–5 °C for 24 h [64]. They obtain spherical nanoparticles (ca. 20 nm) aggregated in long nanofibers/nanotubes. The synthetic procedure was corroborated by Neira-Carrillo et al. [65]. It seems that using a relatively lower concentration of monomer avoids formation of large aggregates. Li et al. manufactured PANI nanodisks by polymerization in water (at 5 °C), at a low concentration (ca. 0.04 M) of aniline and a high (1:0.5) ANI/APS ratio [66]. While the FTIR spectrum shows several bands that could be attributed to PANI, both the UV–vis spectrum and the cyclic voltammogram are quite different than those of PANI. Mahato et al. polymerized aniline at an even lower concentration (0.11×10^{-3} M) and obtained highly crystalline nanospheres [67], which are likely the nucleation centers of nanofiber growth. They seem to use a higher temperature (70 °C) to polymerize in a reasonable amount of time (2 h). They claim that, since aniline polymerization is exothermic, it has to be heated to decrease the rate. Obviously, they confuse thermodynamics with kinetics and it could only be hoped they do not try with higher concentrations of aniline or other exothermic reactions. Wang et al. claimed that aniline concentration is the main factor that determines the morphology of PANI nanostructures [68]. At a lower aniline concentration, PANI nanofibers were formed, while larger PANI aggregates were obtained at a higher aniline concentration. The aggregates can be dislodged using ultrasonic irradiation.

Solution Polymerization Using Oxidants Other Than APS

Most of the synthesis of PANI, including nanostructures, has been performed using APS as an oxidant. However, other oxidants can be used which also promote the formation of PANI nanostructures. Amarnath et al. polymerizes aniline with selenious (H_2SeO_3) acid as an oxidant [69]. The shape of the nano-object depends on the oxidant/aniline mole ratio. When the mole ratio (MR) is very low (0.03–0.125), flakes of PANI are formed. Nanorods (150 nm diameter) are produced at low MR (0.5). At MR = 1, both nanorods and nanospheres were formed. Nanospheres are mainly favored for MR > 1. It should be noted that aniline requires $2.5 e^-$ to oxidize to PANI. The half reaction for the reduction of selenious acid is:



Therefore, 0.5 MR implies 2 mol of e^- (less than the required by stoichiometric ratio) and MR = 1 implies a large excess of oxidant. Moreover, the fate of Se, which is not soluble in water, should be of interest. Lin et al. polymerize aniline (0.5 mmol) using a mixture of FeCl_3 (8 mmol) and CuCl_2 (1 mmol) as oxidants [70]. The stoichiometric ratio for complete conversion of aniline into PANI requires 2.5 mol of electrons (i.e., 2.5 mol of FeCl_3) [71]. They claimed that nanostructures are only formed at an oxidant/aniline ratio between 6 and 10. The authors carry out the polymerization in water but assume that FeCl_3 acts as Lewis acid dopant (Figure 1g,h [65]), disregarding the production of HCl (protons from the polymerization reaction and Cl^- from the reduction of FeCl_3 to FeCl_2). They obtained nanorice structures [72], which are quite useful in photothermal therapy. Another innovative way to produce PANI nanoparticles uses H_2O_2 as an oxidant with an enzyme (glucose oxidase) as a catalyst [73]. The slow reaction produces nanoparticles of up

to ca. 143 nm in diameter (after 162 h). Recently, Zeng et al. manufactured PANI nanobelts using ferric chloride and cumene hydroperoxide as oxidants in the presence of different inorganic acids, which influenced the microstructure [74]. The materials were tested as supercapacitor electrodes using galvanostatic charge/discharge. The best nanomaterial was produced in the presence of sulfuric acid and shows a S_{cap} of 584.1 F g^{-1} (current density of 1 A g^{-1}).

Solution Polymerization with Additives (SPA)

It has been observed that the presence of different ions and molecules induces the formation of PANI nanostructures. Different organic acids can act as additives to produce nanostructured PANI. Among them are AcOH [75], SA [76], DLTA [77], DBSA [78,79], DBSA+NSA [80], NSA [81], CSA [82], PSA [83], and DNSA [84]. In some cases, the organic acid could form micelles alone or as a salt of aniline. However, there is little evidence that micelle, if actually formed, shape and size determine the properties of the PANI nanostructures. Moreover, non-surfactive species: AMPSA [85], AMYGG [86], aminoacids [87] and sulfosalicylate [88] also induce nanostructuring. Moreover, inorganic acids with no amphiphilic nature could also induce nanostructure formation [89]. Other species such as 12-tungstophosphate [90], sucrose stearate [91], sucrose octaacetate [92], AlCl_3 [BuMe2Im]Cl; [BuMePyrrolidin]Cl [93], and β -CD [94,95] also induce formation of PANI nano-objects. Yang et al. polymerized aniline in the presence of 4-sulfobenzoic acid monopotassium salt (4SBAMPS) which delays the decrease in pH due to the polymerization [96]. At a low concentration of 4SBAMPS, PANI plates are obtained which roll into tubes at a higher concentration. The production of oligomers is also monitored and found that oligomers are produced at high pH (>2.6) while the polymer is produced below that pH value. These data confirm the pHDP mechanism. The polymers obtained at a higher pH show lower conductivity. Not only could the shape of the nano-objects be changed by the presence of the additive but also their chirality. Using enantiomerically pure CSA, the nanostructuring effect of the acid also induces chirality of the nanofibers/nanotubes [97–99]. Other chiral acids which induce chirality on the PANI nanostructures are (S)-(-)-2-pyrrolidone-5-carboxylic acid [(S)-PCA] and (R)-(+)-2-pyrrolidone-5-carboxylic acid [(R)-PCA] [100]. Li et al. polymerized aniline in solution in the presence of CTAB [101]. The morphology of PANI nanostructures could be changed from nano-needles or nanowires (50–100 nm in diameter) to hollow microspheres (ca 400 nm in outer diameter) by changing the concentration of the additive. Manohar and coworkers observed the formation of nanofibers by “seeding” with all kind of fibers [102]. However, nanotubes of different materials (e.g., single-wall carbon nanotubes) nanotubes are produced while using nanospheres of another CP (e.g., polypyrrole), PANI nanospheres are produced. Therefore, the seed method belongs to the use of templates. Recently, Xu et al. used IPA as an additive to induce the formation of nanofibrous PANI in a flow reactor [103]. The nanomaterial was tested in an electrochemical cell as a supercapacitor electrode. The nanofibers prepared with 5 wt% IPA show a large specific capacitance ($S_{\text{cap}} = 1082 \text{ F g}^{-1}$).

Solution Polymerization with an External Energy Input

Aniline polymerization is an exothermic reaction. Therefore, no external energy input is required to sustain the reaction. However, the oxidative polymerization of aniline with APS shows an induction period which could take several minutes. Since the induction time disappears when aniline oligomers (e.g., 4ADA) are added [104], it seems that the initial dimerization is a slow reaction. However, the initiation period could be eliminated by light irradiation [105], allowing direct photolithography of PANI. Therefore, instead of slow formation of few nucleation centers, large amount of centers are formed in the irradiated area. Pillalamarri et al. use gamma rays to induce the polymerization of aniline with APS [106]. They obtain nanofibers with diameters that depend on the concentration of aniline and APS. Li et al. use UV light to produce a similar array of nanofibers to use as sensors [107]. On the other hand, Liu et al. use UV light to produce PANI nanofibers

but with the addition of CTAB as a “soft template” [108]. It is unclear if the surfactant is required to nanostructure PANI. Li et al. polymerized aniline with APS and induced the formation of nanostructures by irradiation with UV light [109]. They control the diameter of the nanostructures by changing the oxidant/monomer ratio and the overall concentrations. In that way, they are able to produce nanowires and nanofibers. The most widely used way to induce polymerization externally is the use of ultrasound. Jing et al. manufactured nanofibers by polymerization of aniline with APS and applying ultrasound with a cleaning bath [110]. The diameter of the nanofibers decreases with an increasing APS/ANI ratio. Wang et al. polymerized aniline with APS, adding HCl, citric acid, sulfamic acid and taurine and applying ultrasound [111]. While no nanostructures are observed in HCl, all other additives induce the formation of nanofibers of different sizes. Ganesan et al. use potentiostatic electrochemical oxidation on a Ti ultrasound horn [112]. Applying a short ultrasound pulse after polymerization dislodges the nanoparticles from the electrode, creating a colloidal dispersion. The electrochemical properties of the dispersions are tested by re-depositing the nanoparticles with a binder (Nafion®) by evaporation. While the FTIR and UV-vis spectra are similar to conventional PANI, the cyclic voltammograms show one system of broad peaks without evidence of the two redox processes present in the electrochemistry of PANI [113]. Recently, Qiu et al. used microwaves to induce the formation of PANI nanostructures [114]. The material had 7–10-fold higher electrical conductivity than conventional PANI. Nanosheets were fabricated in weakly acidic media while NFs are formed in highly acidic solutions. Those results are in agreement with the pHDP model. Moreover, both electrical conductivity and electrochemical charge storage are improved when HCl and APS concentrations are increased.

In summary, nanospheres, nanofibers, nanowires, nanobelts, nanodisks, round and square nanotubes, nanobelt and nanodisks can be made by simple oxidative polymerization, changing the conditions.

2.1.2. Solution Polymerization with Polymeric Stabilizer (SPS)

The oldest method to produce polyaniline is polymerization in solution in the presence of a stabilizer [115], where PANI fibers were observed using PEO (30K) as a stabilizer. This method is well known for the fabrication of micrometric and nanometric particles of conventional polymers [116]. When anionic polymers (e.g., acrylic acid) are used to polymerize aniline, the polymer acts as a semi-rigid (due to charge repulsion) template which determines the shape of the PANI, usually a fibril, and not as a stabilizer [117]. Armes and Aldissi use a copolymer, poly(2-vinylpyridine-co-(p-aminostyrene)), as a stabilizer [118,119]. Since the stabilizer contains linked aniline units, it seems that PANI chains graft onto the stabilizer. However, polymerization with APS produces insoluble gels. Therefore, they use KIO₃ as an oxidant which produces nanorice particles, likely due to the dual role (stabilizer and grafting center) of the copolymer. This work was then extended by Armes et al., with a detailed study of the colloidal dispersions produced [120]. At the time, Armes and coworkers thought that this grafting procedure was the only way to obtain colloidal PANI [121,122]. Therefore, Bay et al. use poly(1-vinylimidazole-co-4-aminostyrene) as a stabilizer for polyaniline colloidal nanoparticles [123].

However, Vincent et al. produce PANI nanospheres [124], using a tailor-made polymer with an ethylacrylate/styrene copolymer backbone, with pendant PEO side-chains (SGPEO). It seems that weakly adsorbing PEO allows the fiber to grow while the strongly adsorbing SGPEO inhibits growth and the polymer remains at the nucleation stage. Stejskal and coworkers used PVA (with different remaining acetylation degree) to produce spheroidal nanoparticles of PANI [125,126]. They determine the size of the particles ($R_{\text{hydrodynamic}} = 116 \text{ nm}$) and an estimation of the mean molecular weight of the particles ($520 \times 10^6 \text{ g/mol}$) from a combination of SLS and DLS. Stejskal et al. show that it was possible to stabilize PANI NPs using the current “standard” stabilizer: poly(N-vinylpyrrolidone) (PVP) [127].

Banerjee et al. use poly(vinyl methyl ether) (PVME) as a steric stabilizer of PANI nanoparticles [128]. Since the stabilizer is only slightly soluble in water at 25 °C, they tried

different solvents and oxidants. The best results were obtained with 50% ethanol and APS. Wallace and coworkers produce nanoparticles by electrochemical oxidation of aniline in a hydrodynamic cell [129,130]. Camphorsulfonic acid is used as a dopant. Using the (+) or (−) enantiomer, chiral colloids can be produced. Since ^1H NMR signal of oligoanilines and polyaniline do not give sharp peaks due to slow relaxation, the depletion of aniline can be monitored from the spectra taken at different times [131]. The kinetics shows a longer induction time when APS is used than KIO_3 . However, after induction, the reaction is faster in APS. The addition of PEO as a steric stabilizer does not significantly change the kinetics of the polymerization PANI colloidal dispersions that are obtained by aniline oxidation with APS in an acidic aqueous solution with hydroxypropylcellulose as a stabilizer [132]. Spherical polyaniline particles with small polydispersity are made at 0 °C. On the other hand, at 40 °C the nano-objects are cylinders with coral-like morphology. The difference arises from the faster reaction rate at 40 °C. At 0 °C, faster rates can be achieved by addition of *p*-phenylenediamine. Chin and Park manufacture colloidal dispersions of PANI stabilized by PVME [133]. The more hydrophobic stabilizer allows dispersing the colloid in silicone oil. In that way, an electrorheological fluid with a large ER property (normalized yield stress in an electric field) is produced.

Stejskal review the work on the formation of colloidal dispersions of conducting polymers until 2001 [134]. The role of the steric stabilizer is well accepted in conventional polymers. However, in PANI, Stejskal and Sapurina show evidence pointing out that the stabilizer molecule could act as initiation nuclei of PANI chain self-assembly than be adsorbed on the surface of the nanoparticles [135]. The main evidence is the fact that the stabilizer is required at the beginning of the polymerization when no nanoparticle has been formed to be adsorbed to. Stejskal and Sapurina prepare an IUPAC technical report, where a standard procedure of synthesis of PANI using PVP as a stabilizer was performed by six research groups around the world [136]. Then, the samples were collected and analyzed. The dispersion of properties was low, attesting that the procedure is reproducible.

PANI NP dispersions (with PVP as a stabilizer) are tested in acidic, neutral and alkaline aqueous media, at temperatures of 105 °C (1000 h), sonication, cyclic freezing–melting cycles, or irradiation with UV–visible light [137]. PANI nanoparticles, stabilized with PVA were made into monolayers by the Langmuir–Blodgett technique [138]. PANI NPs stabilized with partially phosphorylated poly(vinyl alcohol) (P-PVA) were prepared by the chemical oxidative dispersion polymerization [139]. The P-PVA acts as a stabilizer and a codopant. The P-PVA/aniline ratio affects the morphology, dispersion stability and electrical conductivity of the nanoparticles. Using a P-PVA/ANI ratio between 50 and 60 wt%, nanospheres were produced which can be dispersed in water and have a high electrical conductivity (up to 7 S/cm). PANI dispersions stabilized by PVP were prepared and thermally characterized by TG–DTA analysis [140]. The composites are stable up to approximately 160 °C. Degradation of PANI chains follows at temperatures exceeding 250 °C. Zimmermann et al. produce colloidal dispersions of PANI nanospheres using PSS as a stabilizer [141]. Interestingly, they did not observe a templating effect of the polyacid, producing nanofibrils, but a stabilizing effect of nanospheres.

Park et al. show that the shape of the PANI nanostructure depends on the concentration of the stabilizer (PVP) [142]. They were able to produce nanospheres, nanorods and nanofibers. The results suggest that PVP adsorbs on the growing chain, inhibiting the growth. At low stabilizer concentrations, PANI could grow into ratio nanostructures with larger aspect ratios: nanorods and nanofibers.

Biopolymers and Smart Polymers as Stabilizers

Anbalagan and Sawant manufacture PANI nanoparticles stabilized by a biopolymer (pectin) to produce a material for supercapacitors [143]. Anjali et al. use the same stabilizer and deposited NPs on paper to use as sensors of bacteria [144]. Gonçalves et al. produce PANI nanoparticle dispersions using gum Arabic and show its biocompatibility [145]. Cruz-Silva et al, manufacture “smart” colloidal dispersions of PANI NPs stabilized by

chitosan (CHI), PVA or PNIPAM [146]. The polymerization was made in weakly acid media using enzymatic oxidation. The NPs stabilized by CHI are stable in acid/neutral media but aggregate in basic media due to the deprotonation of the glucosamine units. The NPs stabilized by PNIPAM flocculate when the LCST temperature of PNIPAM (32 °C) is reached. The colloid size was ca. 50 nm for chitosan or PVA and up to 350 nm for the particles synthesized using PNIPAM. Jasenka' et al. use the enzymatic polymerization method to produce PANI NPs stabilized by CHI or PVA [147]. Abel et al. manufacture colloidal dispersions of PANI NPs stabilized by oxidation with APS in acid media [148]. The dispersions were stabilized by PVP, PNIPAM and hydroxypropylcellulose (HPC). While the PVP-stabilized dispersions are stable at all temperatures, the ones stabilized by PNIPAM flocculate at 32 °C and those stabilized by HPC at 42 °C. The temperatures agree with the LCST transition of the stabilizers. DLS measurement shows the change in size of the nanoparticles upon LCST transition of PNIPAM. Moreover, since PANI absorbs strongly in the NIR range, the thermosensitive dispersions (stabilized by PNIPAM and HPC) also flocculate at 25 °C when irradiated with NIR light due to a local photothermal effect. All the results with these "smart" nanoparticles support the "classic" model of a PANI sphere surrounded by adsorbed hydrophilic polymers which are extended (coil configuration) into the solution. Upon LCST transition, the polymer (e.g., PNIPAM) forms a globular configuration, decreasing the steric stabilizing effect. On the other hand, in the self-assembly model [135], where the hydrophilic polymer is composited with PANI, it is not clear how the LCST transition would decrease the stabilizing effect. The "smart" nanoparticles could have biological applications. Therefore, the interactions with biological entities should be evaluated.

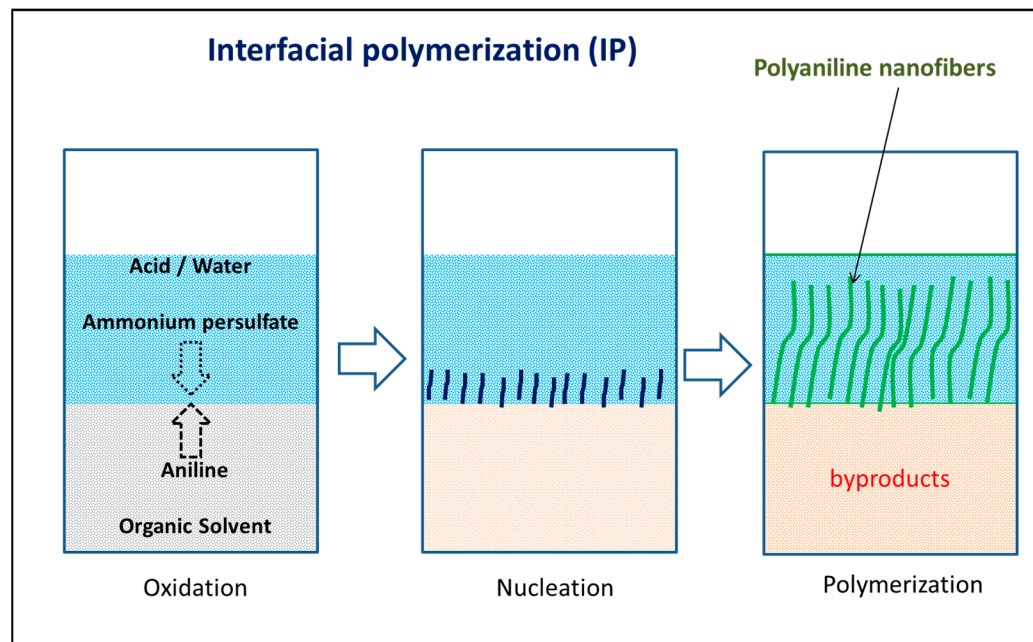
2.1.3. Interfacial Polymerization (IP)

Michaelson and McEvoy polymerize aniline at the interface between an aniline solution in CCl₄ (aided by a surfactant) and an aqueous solution of an oxidant (APS) with acid [149]. Since their interest was to form PANI films, they use conditions where a nanofibrillar mat was produced at the interface. Since CCl₄ is denser than water, the mat floats at the interface and can be attached to an electrode to perform electrochemistry. Moreover, the authors use an additional organic layer (toluene) on top of the water layer, where aniline and oxidant dissolve. Therefore, the reactants are confined in the thin water layer promoting aggregation of the nanofibers into a mat.

Kaner and coworkers use the same technique but with a more polar organic solvent (CHCl₃) [150], which dissolves aniline without surfactants. Only two phases are used and the nanofibers grow into the aqueous layer manufacturing a dispersion. The fibers were characterized by TEM and SEM (backscattered electrons) as well as UV-visible spectroscopy at different pH. The nanofibers have a nearly uniform diameter (30–50 nm) with lengths varying from 500 nm to several micrometers. Upon drying of the dispersions, a nanofiber mat is formed (0.2–5 µm) which was tested as a sensor of acid (HCl) and basic (NH₃) gases. The sensors show clear changes in resistivity due to the protonic acid doping/dedoping. The response time is much faster than PANI films since the mass transport pathlength inside the solid is smaller (30–50 nm vs. 200 nm), and the geometry of the fibers allows for gas intake from the periphery of the fiber, also changing the fiber-to-fiber contact. PANI nanofibers grow at the liquid–liquid interface and are collected in the aqueous phase (Scheme 5). The organic byproducts of the polymerization dissolve in the organic phase.

Taking into account the MTDP and pHDP models, PANI nanofibers should grow at the interface because: (i) the slow mass transport of aniline from the organic solvent to the interface means the local concentration is low, similar to dilution; (ii) using inorganic acids in the aqueous phase (e.g., HCl) which are less soluble in organic solvents means that the local acidity is low, equivalent to a high enough pH, where slow accumulation of nucleates and phenazinic moieties appear. Pramanik et al. studied the interfacial polymerization of aniline in different solvents [151]. They use the difference of solvation parameters [152], to ascertain the effect of the interface on the nanofibers properties. There are little morphologi-

cal properties in the nanofibers. On the other hand, the electronic properties related to their conductivity and UV-vis spectra, the doping measured by quinoid/benzenoid bands in FTIR and the crystallinity (measured by XRD) are strongly affected. It is unclear how the interface affects such properties. One possible explanation is that most of the reaction occurs in the organic solvent, since APS is soluble in different organic solvents, and the aqueous solution only act as reservoir of APS and sink of nanofibers. Su et al. study the effect of acid (HClO_4) concentration and the ratio ANI/APS on the formation of nanofibers by IP [153]. At a low $[\text{APS}]/[\text{ANI}]$ ratio ($\leq 1/4$) and a high HClO_4 concentration (≥ 1 M), uniform PANI nanofibers are produced with a low content of phenazine-like units and ANI oligomers. Therefore, the nanofibers show higher conductivity than typical nanofibers made by IP. Chen et al. manufacture PANI nano-objects by the same interfacial polymerization but adding chitosan to the aqueous solution [154]. The biopolymer will adsorb at the interface and modulates the shape of the nanostructures, at a low (1.5%) concentration of chitosan, nanofibers are produced while only nanospheres are produced at a high (2.5%) chitosan concentration. Nuraje et al. polymerize aniline using FeCl_3 (unknown concentration), a low aniline concentration (ca. 0.01 M) and no acid [155]. They obtained highly crystalline PANI nanorice, likely due to the low concentration and slow reaction. Combining the use of additives with interfacial polymerization, Oueiny et al. obtain nanofibers with benzylphosphonic acid (BPA) and nanotubes with decylphosphonic acid (DPA), both present in the aqueous phase [156]. While at least DPA form micelles, the authors exclude templating by micelles as explanation of the nano-object shape. Zhang et al. polymerize aniline at the interface water/toluene with APS [157]. Two acids were used: CSA and AMPS. Moreover, twin-tailed surfactants were adsorbed at the interface to control the size of the nanofibers. The opposite effect of the surfactants on the size is observed in CSA and AMPS. It is likely that CSA is more amphiphilic, creating a more ordered interphase.



Scheme 5. Reaction steps during interfacial polymerization of aniline to produce PANI nanofibers.

Li et al. use interfacial polymerization of aniline under centrifugal force [158]. They found out that the centrifugal force presses the nanofibers onto the interface, making a fiber mat. Ding et al. use interfacial polymerization with DBSA as acid to produce PANI nanorods [159]. The oxidant/aniline ratio, DBSA concentration and temperature affect the diameters which can be tuned from 40 to 10,000 nm. A lower DBSA concentration and low temperatures produce nanorods of small diameter. Most interfacial polymerization is carried out at flat, quiet interfaces. However, Xing et al. show that nanofibers could

be extended to drops of xylene dispersed in water by strong stirring [160]. The novel method has a larger interface area and could produce larger amount of nanofibers with the same solvent volume. Kamarudin et al. use a homogenizer to stir the mixture, reaching 30,000 rpm [161]. They observe that fast stirring produces shorter and thinner nanofibers. Sun et al. manufacture nanotubes of PANI by IP in the presence of dl-tartaric acid [162]. Above a threshold, the walls of the tubes become thicker and square-shaped nanotubes appear. Dallas et al. use IP to produce PANI nanostructures with SDS (anionic) or DTAB (cationic) additives in the aqueous solution [163]. While IP in the absence of additives gives nanofibers, the presence of these additives induces the formation of small nanospheres. Do Nascimento et al. study the structure and vibrational bands of PANI nanofibers prepared by IP, varying the concentrations of HCl, in the water phase [164]. XRD and SAXS showed that the PANI crystallinity is reduced at high concentrations of HCl. The changes correlate with the occurrence of granular morphology, as observed by SEM. The resonance Raman and FTIR spectra, as well as the EPR data show an increase in the torsion angles of $C_{\text{ring}}-N-C_{\text{ring}}$ segments. It is noteworthy that PANI incorporates chlorine atoms via nucleophilic addition at a high HCl concentration [165]. The steric effect of the chlorine atoms should increase the torsion angle. Zeng et al. manufacture PANI nanostructures with mixed oxidants (APS/ FeCl_3 and APS/ $\text{Cr}_2\text{O}_7^{2-}$) [166]. The use of dichromate, together with APS, produces petal-like nanofibers with a large surface area. Accordingly, the material shows a large specific capacitance (692.4 F/g) in an electrochemical supercapacitor. Cui et al. use a ANI/APS molar ratio of 1/0.25 [167]. Due to the low ANI concentration, petal-like (“cauliflower”) structures are produced. Using PDMS, the nano-object is made hydrophobic. The combination of chemical hydrophobicity and topographic effects (Cassie–Baxter effect [168]) creates superhydrophobic surfaces.

Manuel et al. prepare PANI nanofibers by IP using CCl_4 or CHCl_3 as solvents [169]. They tested the fibers in a lithium ion electrochemical cell with LiPF_6 as an electrolyte. The PANI shows a good charge storage capacity. However, the authors claim that PANI exchange Li^+ during oxidation/reduction while only PF_6^- is exchanged as a counterion of the positively charged oxidized state of PANI [170]. Goel et al. study the FTIR spectra and XRD data of PANI nanofibers at different times during IP and compare the results with conventional PANI [171]. The results suggest that the nanofibers have higher crystallinity than PANI made in solution. Mu, manufacture PANI nanofibers by IP and tested its electrochemical behavior at different pH values [172]. While conventional PANI lost electroactivity at neutral pH, the nanofibers maintain some electroactivity at neutral pH. Jin et al. manufacture PANI nanofibers by IP with the addition of small alcohol molecules which adsorb at the interface between water and the organic solvent [173]. The changes in the interface affect the morphology, microstructure, and electrochemical properties of the PANI NFs. The highest S_{cap} measured was 1042 F g^{-1} (scan rate of 5 mV s^{-1}) and 489 F g^{-1} (current density of 1 A g^{-1}) for the nanomaterial made with ethanol addition.

Other Immiscible Phases

Instead of toxic organic solvents (chloroform, toluene, CH_2Cl_2 , benzene, CCl_4), other phases, immiscible with water, can be used. Akbarinezhad et al. use supercritical CO_2 , which is immiscible with water [174]. PANI nanofibers with ca. 60–80 nm diameter and several micrometer lengths are produced. Gao et al. use an interface between an ionic liquid (1-butyl-3-methylimidazolium hexafluorophosphate ($[\text{C}_4\text{mim}]\text{PF}_6$) and water to produce PANI nano-objects [175]. Instead of nanofibers, small (30–80 nm diameters) nanospheres are produced. Nanoparticles of MgCO_3 and CaCO_3 were dispersed in the aqueous phase of aniline IP [176]. When MgCO_3 nanoparticles were used, polyaniline nanofibers are obtained while nanotubes are produced with CaCO_3 particles. Another immiscible phase is the gas phase. Bhadra and Lee vaporize aniline at 200°C and put the vapor in contact with an acid solution of APS [177]. Nanofibers are produced, which are more soluble than conventionally prepared NF. Yang et al. manufacture nanofibers at the interface between frozen APS/acid/water and aniline/water solution [178]. Different shapes were obtained

changing the concentration or the order of reactant addition. Gao et al. reviewed the manufacture of nano-objects by IP [179]. Dallas et al. wrote an historical perspective of the interfacial polymerization field [180].

2.1.4. Mechanochemical Polymerization

A novel method of aniline polymerization involves the solid-state (solvent-free) polymerization of aniline salts with oxidants (e.g., APS) under mechanochemical conditions [181]. While the solid-state reaction produces a solid, nano-objects can be found during the washing of the solid. Zhou et al. manufacture branched PANI nanofibers by MCP of aniline with Cl_3Fe [182]. The high-surface-area solid shows good properties for energy storage. Du et al. also manufacture branched PANI nanofibers by oxidation of ANI.HCl with $\text{Cl}_3\text{Fe} \cdot 6\text{H}_2\text{O}$ under mortar grinding [183]. The reaction occurs in slurry produced because the iron chloride hydrate melts at 37 °C, which is easily reached by the exothermic polymerization. The MCP is carried with a large ANI.HCl/oxidant ratio which seems required to produce nanofibers. Bhadra et al. manufacture PANI nanospheres (diameter 30–60 nm) by MCP of ANI.HCl with APS under mortar grinding [184]. The polymer inside the NPs shows higher crystallinity than conventional PANI but lower conductivity. Shao et al. manufacture PANI nanospheres (ca. 60 nm) by MCP of ANI.HCl with APS [185]. They studied the effect of water addition to the solid mixture, finding an effect on the doping and electronic properties but not on the nanoparticle size/shape. Bhandari et al. produce PANI nanofibers by MCP of aniline (as sulfate salt) and APS, with the addition of citric acid [186,187]. While it is likely that citric acid affects the nano-structure shape and size, the author's claim that citric acid doped the PANI is unattainable since the polymerization reaction produces sulfuric acid which will protonate the weak citric acid. Acevedo and Barbero show that MCP of ANI.HCl/APS produces a solid consisting of nanoparticles (ca. 70 nm diameter) [188]. From the size and distribution, a S_{BET} of $69 \text{ m}^2 \text{ g}^{-1}$ can be calculated which agrees with the one experimentally measured by Kaner and coworkers [181].

2.2. Manufacturing Colloidal Dispersions of PANI Nano-Objects by Nanoprecipitation of a Preformed Polymer

Since PANI is soluble in some solvents, an additional method to produce nanoparticles involves adding a solution of PANI in a good solvent (e.g., NMP) into a poor solvent of PANI (e.g., water), which is miscible with the good solvent and contains a stabilizer (e.g., PVP). The PANI chains precipitate and form particles where the stabilizer adsorbs and avoids further aggregation. An advantage of this method is that the polymerization and nanoparticle formation steps are separated, allowing detailed characterization of the base polymer. This is relevant since the conditions to produce nanostructures by polymerization (acidity, oxidant/monomer ratio, the presence of template anions or neutral molecules) not only affect the shape of the polymer but also the chemical structure. This method is widely used to produce nanoparticles of conventional polymers (e.g., PLA) and involves nanoprecipitation [189]. It is surprising the limited application of the method to purposely manufacturing PANI nano-objects.

Rubner and coworkers prepare a "solution" of PANI (EB) by diluting a true solution of PANI (EB) in DMF (good solvent) in water (poor solvent) [190,191]. The authors report that the "solutions" were unstable and have to be prepared fresh daily. Since the goal was to self-assemble PANI species by hydrogen bonding or charge, low stability will help the assembly process. It is likely that unstable colloidal dispersions of PANI particles were prepared and assembled. The dispersions were unstable because PANI (EB) is neutral. Therefore, no charge was present and no steric stabilizer was added. In a similar fashion, Li et al. mix a solution of PANI in formic acid (good solvent) with acetonitrile (poor solvent) [191]. They produce a dispersion of PANI NPs which are then deposited electrophoretically on Pt or ITO. In this case, the dispersion is more stable since the nanoparticles are charged by doping/protonation of formic acid which also provides the electrolyte. The double layer around the charged PANI nanospheres should be large since acetonitrile has a relatively low

dielectric constant. Repulsion of the equally charged double layers of different nanoparticles avoids aggregation.

On the other hand, Abel et al. studied in detail the manufacturing process of PANI nanospheres by mixing a solution of PANI (EB) in NMP (good solvent) with water (poor solvent) which contains PVP (a steric stabilizer) [192]. The size of the NPs is determined by the concentration of PANI in NMP and the amount of solution in NMP added to the water. Nanospheres from 40 to 250 nm can be produced in that way. Since the emeraldine base form is used, it is possible for PANI chains to somewhat coil and produce small nanoparticles of mean-molecular-weight PANI. Nanoparticles can be made by mixtures of PVP with other stabilizers (e.g., PNIPAM) but not without PVP and the size depends also on the ratio PVP/PNIPAM. The method was used to produce fluorescent NPs by nanoprecipitation of PANI functionalized with fluorescent groups (dansyl).

3. Applications of Nano-Objects Synthesized by Template-Free Polymerization

The main goal for template-free manufacturing of PANI nano-objects is to produce technological applications. In various applications (e.g., double-layer capacitors), the specific surface area of the nano-object ensemble (e.g., nanofiber mat) is a relevant parameter. In Figure 2 is shown the calculated S_{BET} for PANI nanospheres or nanocylinders (nanorods, nanofibers) of different diameters. The Area/volume ratio (which is related to S_{BET} through the density) only depends on the radius of the object. As can be seen, nanospheres have a larger area than nanocylinders for the same diameter but the difference decreases with diameter. Moreover, quite small nanoparticles have to be manufactured to obtain large S_{BET} values. In the case of nanospheres, a particle of 10 nm in diameter has a S_{BET} of $400 \text{ m}^2 \text{ g}^{-1}$, while a nanocylinder of 10 nm in diameter has only a S_{BET} of $267 \text{ m}^2 \text{ g}^{-1}$. However, the calculation assumes a compact nano-object while solid PANI is made of polymer chains with a non-compact interface. Therefore, experimental values of S_{BET} could be larger.

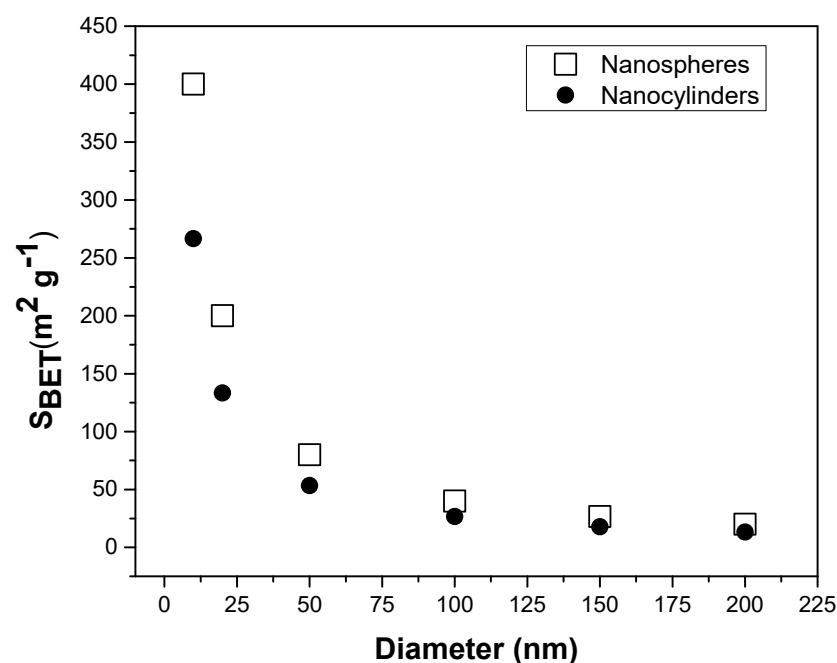


Figure 2. Calculated S_{BET} of PANI nano-objects as a function of the diameter of the object.

Another parameter of interest is the time required for a mobile species (counterion, analyte, adsorbate) to reach the center of the nano-object. This parameter is related with the response time of batteries and supercapacitors (where redox pseudocapacitance has a major contribution), response time of sensors and loading time of adsorption nanomaterials.

In Figure 3 is shown the diffusional response time of the nanospheres/nanocylinders for different diffusion coefficients (typical of solids). In all cases, the response time

is below one second, even for relatively large diameters (200 nm) and slow diffusion ($D_o = 10^{-10} \text{ cm}^2 \text{ s}^{-1}$). Therefore, the use of nano-objects ensembles could improve significantly the behavior of the device, even for larger diameters.

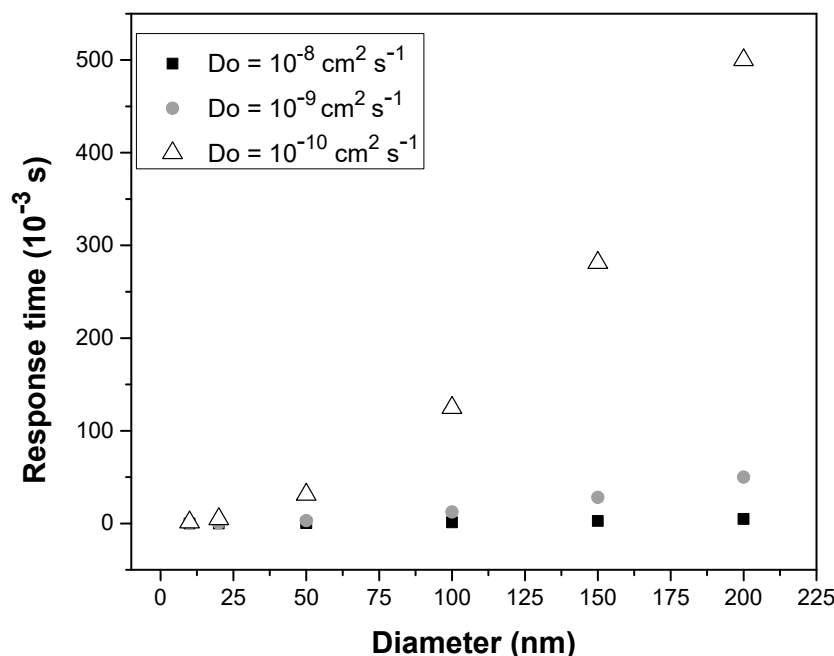


Figure 3. Calculated diffusional response time of nanospheres/nanocylinders as a function the diameter of the object.

Subsequently, selected applications in each different field will be described.

3.1. Sensors

Polyaniline is a material widely used for sensors [193–195]. It can be used as conductor in electrochemical or resistive sensors. Moreover, the electroactivity and UV–visible spectra depend on pH. The surface can be modified by simple organic chemistry reactions to bind enzymes, antibodies, aptamers, etc. Using PANI nanomaterials, it is possible to increase the surface area (Figure 2) and decrease the response time (Figure 3). Indeed, the first application of PANI nanofibers was as an ammonia resistive sensor [150], where the time response was faster than for PANI films. PANI nanofibers prepared by the MTDP method were used as reductants of Ag^+ to produce Ag^0 nanoparticles [196]. The large surface area of the nanofiber mat allows producing small and dispersed Ag nanoparticles which show SERS activity. Popov et al. manufacture PANI nanofibers by IP [197]. They combine the NF with rGO, Nafion[®] and glucose oxidase to manufacture electrochemical glucose sensors. Nate et al. manufacture PANI nanofibers loaded with cobalt oxide (Co_3O_4) nanoparticles by IP [198]. To that purpose, Co_3O_4 NPs are dispersed in the aqueous phase of IP. Thin films of the nanomaterial are then deposited onto GC by drop casting. The films are used to detect electrochemically antimalarial drugs, where the PANI NF mat act as conductive matrix and the cobalt oxide as electrocatalyst. Zou et al. produce PANI nanotubes by SP and combine with graphene and aramid nanofibers to produce aerogels [199]. The elastic and conductive aerogels show excellent properties as pressure sensors. Thakur et al. manufacture biocompatible PANI nanospheres by SPS using a biopolymer (pectin) [200]. The colloidal dispersion is used to sense the growth of *Escherichia coli* through the change in visible spectra of the emeraldine base (blue) to emeraldine salt (green). The organic acids produced by the bacteria protonate the PANI backbone. Zhao et al. manufacture PANI nanofibers by IP [201]. An enzyme (glucose oxidase) was covalently bonded to the NFs by amidation and used as an amperometric sensor of glucose. The field of nanostructured conducting polymers applied in sensors was previously reviewed [202].

3.2. Electrochemical Energy Storage

Energy storage applications (batteries/supercapacitors) of electroactive PANI require preparation of solid electrodes with a large surface area/small solid size and macro/mesoporosity [203]. The large surface area (Figure 2) allows development of a double layer for charge storage in supercapacitors while the small solid size of the nano-objects decrease the pathlength of slow mass transport of ions inside the solid (Figure 3), which is the rate controlling processes in batteries. Moreover, macro/mesoporosity is required to provide/sink ions in the solution (fast mass transport). Therefore, hierarchical structures are especially suited for energy storage [204]. Nanofibers mats or nanocomposites could fulfill those requirements [205]. Kim et al. manufacture PANI nanofibers by MTDP and disperse them in a polyelectrolyte (Nafion®) [206]. The manufactured supercapacitor show good specific capacitance and high flexibility. Gao et al. produce nitrogen-enriched carbon nanofibers by carbonization of PANI NFs [207]. The polymeric nanomaterial was made by SP using the MTDP method. The resulting N-enriched (7.59 at %) carbon nanofibers have diameters in the range 100–150 nm with a S_{BET} of $915 \text{ m}^2 \text{ g}^{-1}$. The S_{cap} is of 172 F g^{-1} (at 2 mV s^{-1}). It shows a good cycling stability (89% S_{cap} retention after 5000 cycles). Udayan et al. manufacture PANI nanofibers by IP, and combine them with a MOF (ZIF-8) to produce a flexible electrode material for supercapacitors [208]. Due to its hierarchical structure, ZIF-8/PANI has a S_{BET} of $610.8 \text{ m}^2 \text{ g}^{-1}$ and a S_{cap} of 395.4 F g^{-1} (at a current density 0.2 A g^{-1}). The field of application of PANI, including nanomaterials, in supercapacitors has been reviewed [209].

3.3. Corrosion Protection

It is well known that PANI coatings protect metals from corrosion [210,211]. However, since PANI is not soluble in common solvents, the formation of coatings on large surfaces is difficult. Using colloidal dispersions is a well-known method to produce protective metal coatings. Therefore, dispersions of PANI nano-objects could be used to produce protective coatings. Fuseini et al. deposited PANI colloids by electrophoresis onto copper [212]. The colloidal dispersions were made by nanoprecipitation from a formic acid (good solvent) solution of PANI using ACN as poor solvent and ultrasonication to aid the dispersion. The dispersion is stabilized by protonation as shown by zeta potential measurements ($\zeta = +32.9 \text{ mV}$, $D_h = 542 \text{ nm}$). The charged colloids are driven by the electric field (15 V) into the negative Cu electrode. The produced coating resembles PANI chemical or electrochemical films, suggesting that the colloidal particles aggregate during deposition. Indeed, the PANI coating acts as a barrier for electrolyte reaching the Cu, inhibiting the metal corrosion. Abel et al. synthesize PANI nanofibers by IP [213]. Then, the NFs were surface functionalized by addition [214], of different nucleophiles, producing nanofibers with different surface properties. While PANI NF dispersions are stable in acid media due to charge repulsion of the protonated fibers, they aggregate into porous mats at neutral pH. Therefore, conducting mats of functionalized nanofibers can be deposited onto interdigitated metal electrodes. The modified electrodes show different conductivity changes when exposed to volatile organic contaminants. Combining the signal of several electrodes, electronic noses can be manufactured. While conventional PANI lost electroactivity at neutral pH, the nanofibers maintain some electroactivity at neutral pH.

3.4. Biomedical Applications

While electronic properties are relevant for battery or sensor research, biocompatibility is required to use nanofibers in biomedicine (e.g., photothermal therapy). Yslas et al. studied the toxicity and teratogenicity, using toad embryos, of PANI NF produced by IP (using HCCl_3 as organic phase) [215]. The NF shows low toxicity and dose-dependent teratogenicity. Ibarra et al. measure the toxicity and teratogenicity of PANI NPs, stabilized by PVP. Interestingly, while PANI seems innocuous, low-molecular-weight PVP (30 K) shows some deleterious effects. Ibarra et al. synthesize PANI nanospheres by SPS [216]. The NPs show in vitro (HeLa cell line) and in vivo (mouse) photothermal activity against human

tumors. Kašpárková et al. manufacture PANI colloids stabilized with CHI and sodium hyaluronate (SHA) [217]. They show that they are only weakly cytotoxic against mouse fibroblasts while they show clear antibacterial activity. Molina et al. manufacture PANI nanospheres (ca. 200 nm) by solution polymerization in the presence of a steric stabilizer (PVP) [218]. The stable dispersions are absorbed into macroporous hydrogels of PNIPAM made by cryogelation. The PANI NPs, retained inside the gels, absorb electromagnetic radiation (e.g., NIR light) and heat up, triggering the volume collapse of the thermosensitive hydrogel. Jasenka' et al. manufacture PANI NPs stabilized by CHI or PVA [147]. The NPs showed in vitro antioxidation activity. Therefore, the NPs were applied to reduce oxidative stress and inhibit the production of ROS by neutrophils. The NPs also reduce the production of inflammatory cytokines by macrophages.

Ghosh et al. manufacture PANI (and PEDOT) nanofibers by SP using an additive (CTAB) [219]. Thin films were produced by drop casting. The films exhibited strong antimicrobial activity, under UVA irradiation, against Gram-positive (*Staphylococcus aureus*) and Gram-negative (*Escherichia coli*) bacteria. Pang et al. use PANI NPs, bearing vinyl groups, to crosslink hydrogels [220]. The nanocomposites show good mechanical and antibacterial properties which allow their use in wound dressing. The field of stimuli-responsive nanogels, which include those loaded with PANI, has been already reviewed [221].

3.5. Optoelectronics

Since nanoparticles are dispersible in organic solvents, nanocomposites of soluble dielectric polymers and PANI nano-objects can be made by casting films from mixed solutions. Araujo et al. synthesize nanofibers by IP (CH_2Cl_2 (with SDS)/water [222]. The nanofibers were dispersed in butanone and mixed with a solution of PMMA in the same solvent under sonication. By evaporation of the solvent, homogenous nanocomposite films can be casted. Ghaleghafi et al. used three different methods to produce nanocomposites of 2D MoS_2 and 1D PANI (nanofibers) [223]. One of the methods involve synthesizing PANI nanofibers and mixing with nano MoS_2 (synthesized by hydrothermal (HT) reaction of molybdate ion with thiourea). Another involves the HT synthesis of nano MoS_2 in the presence of PANI nanofibers. The optoelectronic properties are poorer than the nanocomposite made by in situ polymerization of aniline in the presence of nano MoS_2 , suggesting that mixing the nanomaterials produce phase separation. On the other hand, PANI nanofibers likely degrade under the hydrothermal conditions (210 °C for 24 h) used to produce nano MoS_2 . Yarmohamadi-Vasel et al. manufacture PANI nanofibers by MCP using iron chloride as an oxidant [224]. The NFs are combined with TiO_2 NPs, in different architectures, producing photovoltaic cells. The deposit of PANI NFs acts efficiently as the hole-injection layer.

3.6. Microwave Absorption

As an electronic conductor, PANI interacts strongly with oscillating electromagnetic fields. In that way, it can absorb and reflect microwaves [225]. Using PANI dispersion allows producing composites with structural polymers. Zhang et al. manufacture PANI nanoparticles by SP with polymer (PVP) stabilizer [226]. PANI nanoparticles exhibit very strong reflection losses (up to -40.5 dB at 5.8 GHz) with a wide bandwidth (up to 3.2–18 GHz over -10 dB). The values are comparable to magnetic particles. Yang et al. manufacture nanorod-coated PANI microtubes [227]. The hierarchical structures are made by SP using SDS as an additive and adjusting the HCl concentration. The material show a large absorption of -43.6 dB (1.55 mm thick) and a wide absorption band of 5.84 GHz. Su et al, manufactured PANI nanotubes by SP [228]. To form the nanotubes, acetic acid was used as an additive. Since ferric chloride is added to the polymerization solution, the polymer nanotubes retain iron. Upon carbonization in the absence of oxygen, nitrogen enriched carbon nanostructures loaded with iron are produced. The presence of Fe improves the microwave absorption properties of carbon. The reflection loss of the Fe/carbon fibers is of -44.09 at 6.62 GHz, with a bandwidth of 6 GHz.

3.7. Adsorption of Contaminants

The chemical nature of PANI, with aromatic rings, hydrogen bonding centers and positive charges (cation radicals) allows interaction with charged, hydrogen bonding donor/acceptors and anions. PANI nanomaterials show large surface areas (Figure 2) to interact with a large molecules (e.g., proteins). On the other hand, small molecules could penetrate inside the solid nanomaterial and the short pathlength allows for short response times (Figure 3). Bayat et al. manufacture PANI nanofibers by emulsion polymerization using CTAB [229]. Then, SiO_2 is formed onto the nanofibers and linked to PANI using formaldehyde. The nanocomposite is dispersed in a PVA/CHI solution to produce fibers by electrospinning. The presence of PANI promotes the adsorption of anionic dyes on the cation radical charges of the CP backbone. Lyu et al. use the same property of PANI to adsorb acid red G dye on PANI nanofibers [230]. PANI nanofibers were produced using FeCl_3 as an oxidant and varying the reaction temperature and aniline/to oxidant ratio (R_{AOx} from 1:2 to 1:12). The authors use a relatively large acid (HNO_3) concentration (ca. 0.4 M) and assume that the counterion of the as produced PANI is NO_3^- . However, the aniline concentration is ca. 0.18 M. Therefore, chloride (from FeCl_3) concentration is in the range 1 (ratio 1:2) to 6.5 (ratio 1:12) M and Cl^- should be dominant as counterion. The retention of the anionic dye reaches up to 491 mg g^{-1} for a material produced at 20°C with a R_{AOx} of 1:4. Such material has a S_{BET} of $25 \text{ m}^2 \text{ g}^{-1}$. The adsorbed dye could be removed by deprotonation of PANI and the removal is reversible for 10 cycles.

3.8. Photothermal Applications

PANI absorbs light in the UV–visible–NIR range [231], heating up the polymer [232]. Additionally, an alternating electromagnetic field (RF or MW) interacts with the charge carriers, creating Eddy currents inside the conductive nanoparticles which locally heat up them. It has been shown that PANI have to be in the conductive state (protonated) to interact with electromagnetic field (such as MW or RF), but NIR light is also absorbed by the deprotonated state [233]. Abel et al. grow thermosensitive hydrogels around PANI nanofibers (made by IP) and nanospheres (made by SPS with PVP) [234]. The LCST transition of the hydrogel matrix was induced by application of RF (30 kHz, 1 kW) or MW (2.4 GHz, 700 W). Bongiovanni Abel et al. synthesize PANI nanospheres by SPS, using a thermosensitive polymer (PNIPAM) as a stabilizer [235]. The nanoparticles are then used to stabilize Pickering emulsions of water immiscible organic solvents. Upon heating, the nanoparticles become destabilized and the emulsion breaks. Moreover, PANI NPs could be locally heat up by applying RF, inducing the emulsion break. Dong et al. synthesize PANI nanofibers by IP [236]. The nanomaterial is dispersed in epoxy curing mixture and the healing of coating damage is activated photothermally by NIR (808 nm) light. PANI nanofibers absorb the light, and heat up, increasing the rate of epoxy curing.

3.9. Electrorheological Fluids

Since conductive PANI nanoparticles bear charges, they will be affected by strong electric fields. Specifically, the flux of a charged colloidal dispersion is hindered by the electrostatic force exerted by the external field on the colloid. Such electrorheological effect could be used in non-mechanical brakes and variable transmission devices [237]. Quadrat and Stejskal reviewed the application of PANI nano-objects, manufactured without templates, in electrorheology [238].

Wang reviewed the methods of fabrication of PANI nanofibers, including template-free processes [239]. He also described and discussed technological applications of PANI nanofibers.

4. Conclusions

The work reviewed suggests that it is possible to produce a variety of different shaped/sized PANI nanoparticles by polymerization or nanoprecipitation of the preformed polymer, without using templates. The widely used oxidative polymerization of aniline in

solution (SP) produces nano-objects (e.g., nanofibers) by controlling the polymerization conditions. Two models are proposed to explain the formation of nano-objects, instead of macroscopic aggregates. One explains the formation of nanofiber by the restrictions in mass transport in a non-stirred solution (MTDP). In those conditions, fast nucleation and slow growth give rise to 1D nanostructures. The other model (pHDP) is based on the effect of pH during polymerization. At high pH, non-only linear (head-to-tail) polyaniline oligomers are formed but also chains with *ortho* substitutions and phenazinic rings are produced. The non-linear chains show lower conductivity and crystallinity but self-assemble, giving rise to nanofibers and nanotubes. On the other hand, the presence of aniline oligomers (e.g., 4-aminodiphenylamine) also makes the initiation/nucleation step, promoting the formation of 1D nanostructures. A variety of ions (e.g., SDS) or neutral species (e.g., IPA) could act as additives promoting the formation of nano-structures and controlling the shape/size of the nano-objects.

In addition to the formation of nano-objects, the manufacturing of high-solid-content colloidal dispersions of PANI nanoparticles requires stabilization. Hydrophilic polymers (e.g., PVP) which adsorb on the surface of the particles could act as steric stabilizers in aqueous solutions. Stable dispersions of spherical nanoparticles, produced by conventional solution polymerization, could be manufactured using such polymers, including biopolymers (e.g., pectin) or biobased polymers (e.g., hydroxypropylcellulose). Smart polymers (e.g., PNIPAM) have also been used as stabilizers of PANI nanoparticles. The polymer chains react to external stimuli (e.g., temperature) by changing its spatial conformation from coil to globule (LCST transition). Since the stabilizing effect requires the polymer chain to be unfolded in solution, the colloidal dispersions can be flocculated by increasing the temperature above the LCST. The nanoparticles can be redissolved by cooling with string stirring. Moreover, by irradiation with electromagnetic radiation (e.g., NIR light), which is absorbed by PANI, the flocculation can also be induced since the PANI core heats up and triggers the LCST transition of the PNIPAM stabilizer shell.

The polymeric stabilization could also be used to produce PANI nanospheres by nanoprecipitation. Mixing a solution of PANI (EB) in a good solvent (e.g., dimethylformamide) with a poor solvent (e.g., water) induces the precipitation of PANI. Since the solvents are miscible, the good solvent is diluted in the poor solvent and the interactions with the polymer are weakened, promoting chain aggregation. The formed nanoparticles aggregate into macroscopic precipitates. However, if the poor solvent contains a steric stabilizer (e.g., PVA) or immobile charges are generated (e.g., by protonation), stable dispersions will be produced. Since the process is controlled by solubility equilibrium and mass transport, the size of the nanoparticles depends on the number of nuclei and the amount of available stabilizer. Therefore, small (down to ca. 40 nm) nanoparticles can be produced. The method has been scarcely used, when could be used to manufacture nanoparticles from PANI, copolymers and functionalized polyanilines [240]. Geometrical considerations preclude the formation of small nanoparticles of a high-molecular-weight rigid polymer, since the polymer could not fold into a small globule. Since PANI grows in the pernigraniline state, which is highly conjugated and rigid, the mean chains ($M_n = 96800$ g/mol) could not produce nanoparticles smaller than 280 nm. Therefore, very small nanoparticles (e.g., single-crystal nanorices) are likely made of low-molecular-weight chains. On the other hand, PANI chains in the emeraldine form are also rigid but the angle in the Ar-NH-Ar diphenylamine unit makes the polymer take a ring-like shape with a smaller diameter (down to 90 nm). These considerations explain why small-diameter (<50 nm) nanotubes can be built. The formation of nanospheres by precipitation of PANI (EB) from solution could be explained due to the relaxation of that constraint.

In summary, nanospheres can be prepared by solution polymerization with stabilizers and nanoprecipitation of preformed PANI from solution. Nanofibers and single crystals (nanorices) are usually produced by interfacial polymerization. Nanotubes are produced by solution polymerization with varying pH or using additives. Other shapes can be produced

(petal-like or square nanotubes, nanorice single crystals, nanobelts, nanodisks, etc.) by changing some parameters of the polymerization.

5. Future Directions

Several synthetic methods at solid interfaces produce polyaniline nanoparticles without templates: electrochemical [241], chemical [242], or photochemical polymerization produce solid aggregates which do not disperse in the solvent. While such behavior is useful to produce nanostructured solid materials, it precludes the application in dispersed form. A post-polymerization dispersion step, using polymeric stabilizers (e.g., PVP) and fast stirring or ultrasound will enable to produce stable dispersions and extend solid-state methods (including mechanochemistry) to the formation of dispersed PANI nano-objects.

While nanoprecipitation is a well-known method to produce nanoparticle dispersions of common polymers, it has been seldom used to produce PANI colloidal dispersions. Biopolymers (e.g., CHI) and even biomacromolecules (proteins, polysaccharides, and nucleic acids) could be used as stabilizers. In that way, biocompatibility will be improved and new properties (e.g., immunogenicity) could be incorporated. It has been shown that conducting polymers functionalized with solvophilic groups could act as polymeric stabilizers of nano-objects (e.g., carbon nanotubes [243,244]). In the case of PANI nano-objects, the use of such electronic conductive stabilizers should improve the bulk conductivity of films since the electron hopping between nano-objects should be less hindered than with a dielectric polymer stabilizer.

Interfacial polymerization is the preferred technique to produce PANI nanofibers. However, usually solvents which are harmful and/or environmentally deleterious (e.g., chloroform) are used. While other immiscible phases, such as supercritical CO₂ [174] or ionic liquids [175] have been applied, they are usually expensive and/or of complex operation. On the other hand, common organic solvents with a low environmental impact [245], which are immiscible with water, could be applied. Moreover, even solvents soluble in water (e.g., acetonitrile) or even pure liquid aniline form a separated aqueous phase when put in contact with concentrated aqueous solutions of hydrophilic species (e.g., CaCl₂). Using those kinds of solvents, a more ecofriendly way to produce PANI nano-objects by interfacial polymerization could be devised.

The mechanism of template-free polymerization on solution is still unclear and further investigation on the subject could provide useful information. However, from the technological point of view, the setting of clear procedures to produce PANI nano-objects in a reproducible way seems more relevant. Such an endeavor requires re-studying published work where sometimes the experimental details are not complete and/or the results could not be reproduced by unknown reasons. However, the systematic record of testing detailed synthetic procedures to produce all possible shapes (nanospheres, nanorice, nanobelts, nanofibers, nanotubes, nanodisks, etc.) would be very useful towards application of PANI nano-objects.

Once stable PANI colloidal dispersions are obtained, they can be used to build larger structures or nanocomposites. In general, nanocomposites have usually been produced by in situ polymerization of aniline inside the matrix [246], or in the presence of the dispersion of another nanomaterial [247]. While the method has been widely used [248–250], it precludes a complete characterization of the in situ produced nano PANI. Indeed, the materials produced by in situ polymerization of aniline inside hydrogels have usually been considered a kind of blend (semi-interpenetrated networks) [251]. It was experimentally shown that they are nanocomposites with PANI nanoparticles filling the pores of the polyacrylamide hydrogel [252]. However, the semi-interpenetration model is still believed to be true since the true nature of the PANI inside the matrix is not simple to characterize [253]. Therefore, even when manufacturing solid structures (thick and thin films, porous materials, etc.) is the main goal, colloidal dispersions could be useful. The building process requires assembly of the particles into a stable solid. In that sense, layer-by-layer self-assembly [254], the method pioneered by Rubner and coworkers using unstable PANI

“solutions” in water [190], allows building films with controlled thickness. While they use hydrogen bonding as self-assembly interactions, protonated PANI (positive charged) could be assembled with negative polyelectrolytes. Moreover, PANI nanoparticles could be stabilized with polymers bearing charges (e.g., polyelectrolytes) or hydrogen bonding donors (e.g., CHI) or acceptors (e.g., PVP). By preparing nanoparticles, by in situ polymerization or nanoprecipitation, bearing both kinds of stabilizers, self-assembly of PANI multilayers can be achieved [255]. On the other hand, while each adsorption step adds mass to the film, it is not clear that nanoparticles behave as macromolecules [256]. In larger colloids, which can be observed in situ by optical microscopy, bidimensional (2D) covering resembling molecular adsorption was found [257]. In most applications of nanostructured films (e.g., supercapacitor electrodes), the 2D self-assembly should have similar properties than the multilayer.

Other ways to produce structures from dispersions involve electrophoresis, drop casting, and spin coating. Electrophoresis has only been used to produce films of undefined nanoparticles made by nanoprecipitation (without stabilizer [191]). On the other hand, it has been applied to deposit 1D materials, such as carbon nanotubes [258], and metal nanorods [259], as well as 2D materials, such as graphene [260]. The higher dimensionality of the nano-objects induces multiple dispersion interactions which fix the nanomaterial to the surface. PANI nano-objects strongly absorb light in the UV–visible–NIR wavelength range (200–1600 nm). On the other hand, heat conduction out of the nano-object is hindered by the low thermal conductivity of the surrounding media. Therefore, the nano-objects could reach higher temperatures than thick PANI films. Such an effect has been used by Kaner and coworkers to flash weld PANI nanofibers [261]. Moreover, PANI thin (200–300 nm) have been structured by laser ablation (DLIP [262]), or transferred by LIFT [263], using the photothermal effect. Applying such methods to different PANI nano-objects could be used to manufacture hierarchical structures and complex devices containing PANI nano-objects. When polymers are used as stabilizers, the film formed by aggregation of nano-objects contains the stabilizer as an interlayer.

Such a layer affects the properties (e.g., conductivity) and its nature depends on the drying process. The effects of the drying process on the film structure have been studied [264], and the results could be used as guidelines to improve the reproducibility and properties of films produced from colloidal dispersions of PANI nano-objects. On the other hand, macroscopic structures such as thick films/mats are likely the most useful form of nanomaterial for technological applications, such as supercapacitor electrodes and adsorption membranes. Early on, it was demonstrated that interfacial polymerization produces a porous membrane made of PANI nanofibers [149]. The method should be developed further and include the incorporation of other nanomaterials (e.g., carbon nanotubes). Another way, extensively used in the formation of carbon nanotubes and cellulose nanofibers mats [265], involves the deposition from vacuum filtration through a fine pore membrane. The method can be easily applied to PANI nanofibers, nanotubes or even nanorods. The thickness of the mat can be controlled by the amount of dispersion filtered and different 1D nanomaterials can be combined.

The low-cost, easy and reproducible synthesis of PANI nano-objects suggests their use as templates of solids to form nanoporous materials. Other well-known nanomaterials, such as silica nanospheres, have been used to template pores into solid materials [266], by in situ formation of the solid around the particles. However, the removal of the template requires corrosive solutions (e.g., HF). On the other hand, PANI nano-objects can be removed by dissolution (e.g., in NMP) for soft materials (e.g., crosslinked polyacrylamides) or by calcination for heat-resistant solids (e.g., metal oxides). Using PANI nanofibers, it is possible to template open pores in the solid. Such porosity is required for most chemical applications (e.g., adsorption of contaminants from solution) where the species have to reach the inside of the solid. Since the solid itself could have a porosity level, hierarchical structures can be formed.

Funding: The work was funded by SECYT-UNRC (SSPR), FONCYT (PICT 2450/2019, PICT II Salto Institucional) and CONICET (PUE IITEMA).

Conflicts of Interest: The author declares no conflict of interest.

Abbreviations

4ADA	4-aminodiphenylamine
AcOH	acetic acid
AMPSA	2-acryamidopropansulfonic acid
AMYGG	Acid Mordant Dark Yellow GG
ANIHCl	anilinium hydrochloride
APS	Ammonium persulfate
CHI	chitosan
CSA	camphorsulfonic acid
CTAB	cetyltrimethylammonium bromide
DBSA	dodecylbenzenesulfonic acid
DLIP	direct laser interference patterning
DLS	dynamic light scattering
DLTA	(DL) tartaric acid
DNSA	dinitrosulfosalicylic acid
DTAB	dodecyltrimethylammonium bromide
EB	emeraldine base
ES	emeraldine salt
GC	glassy carbon
HA	hyaluronic acid
IP	interfacial polymerization
LCST	lower critical solution temperature
LIFT	laser-induced forward transfer
MCP	mechanochemical polymerization
MM2	molecular mechanics (version 2)
MOF	metal organic framework
MTDP	Mass Transport Determining Polymerization
MW	microwaves (0.5–20 GHz)
NIR	near infrared range (800–1600 nm)
NMP	N-methylpyrrolidone
NPT	nanoprecipitation
NSA	naphtalenesulfonic acid
PANI	polyaniline
PANI(EB)	polyaniline (emeraldine base form)
PEO	poly(ethylene oxide)
pHDP	pH determined polymerization
PN	pernigraniline base
PNIPAM	poly(N-isopropylacrylamide)
PSA	pyrenesulfonic acid
PVA	poly(vinylalcohol)
PVP	poly(vinylpyrrolidone)
RF	radiofrequency (10–100 kHz)
SA	salicylic acid
SAXS	small-angle X-ray scattering
S_{BET}	specific surface area ($\text{m}^2 \text{g}^{-1}$) measured by nitrogen adsorption isotherm
S_{cap}	specific capacitance (F g^{-1})
SDS	sodium dodecyl sulfate
SEM	scanning electron microscopy
SERS	surface enhanced Raman spectroscopy
SGPEO	star-grafted PEO chains on ethylacrylate/styrene linear copolymer
SLS	static light scattering

SP	solution polymerization
SPS	solution polymerization with stabilizers
UVA	ultraviolet light (315–400 nm)
XRD	X-ray diffraction
ZIF-8	zeolitic imidazolate framework-8
β-CD	β-cyclodextrin

References

1. Reynolds, J.R.; Thompson, B.C.; Skotheim, T.A. *Handbook of Conducting Polymers*, -2 Volume Set; CRC Press: Boca Raton, FL, USA, 2019.
2. Shirakawa, H.; Louis, E.J.; MacDiarmid, A.G.; Chiang, C.K.; Heeger, A.J. Synthesis of electrically conducting organic polymers: Halogen derivatives of polyacetylene, (CH)_x. *Chem. Commun.* **1977**, *16*, 578–580. [[CrossRef](#)]
3. Runge, F.F. On some products of coal distillation. *Ann. Phys. Chem.* **1834**, *31*, 513–524. [[CrossRef](#)]
4. De Surville, R.; Jozefowicz, M.; Yu, L.T.; Pepichon, J.; Buvet, R. Electrochemical chains using protolytic organic semiconductors. *Electrochim. Acta* **1968**, *13*, 1451–1458. [[CrossRef](#)]
5. Macdiarmid, A.G.; Chiang, J.C.; Richter, A.F.; Epstein, A.J. Polyaniline: A new concept in conducting polymers. *Synth. Met.* **1987**, *18*, 285–290. [[CrossRef](#)]
6. Kulkarni, V.G.; Campbell, L.D.; Mathew, W.R. Thermal stability of polyaniline. *Synth. Met.* **1989**, *30*, 321–325. [[CrossRef](#)]
7. Sapurina, I.; Riede, A.; Stejskal, J. In-situ polymerized polyaniline films—3. Film formation. *Synth. Met.* **2001**, *123*, 503–507. [[CrossRef](#)]
8. Wang, J.; Zhang, D. One-dimensional nanostructured polyaniline: Syntheses, morphology controlling, formation mechanisms, new features, and applications. *Adv. Polym. Sci.* **2013**, *32*, E323–E368. [[CrossRef](#)]
9. Virji, S.; Fowler, J.D.; Baker, C.O.; Huang, J.; Kaner, R.B.; Weiller, B.H. Polyaniline nanofiber composites with metal salts: Chemical sensors for hydrogen sulfide. *Small* **2005**, *1*, 624–627. [[CrossRef](#)]
10. Jiang, H.; Ma, J.; Li, C. Polyaniline-MnO₂ coaxial nanofiber with hierarchical structure for high-performance supercapacitors. *J. Mater. Chem. A* **2012**, *22*, 16939–16942. [[CrossRef](#)]
11. He, J.; Liang, Y.; Shi, M.; Guo, B. Anti-oxidant electroactive and antibacterial nanofibrous wound dressings based on poly(ε-caprolactone)/quaternized chitosan-graft-polyaniline for full-thickness skin wound healing. *Chem. Eng. J.* **2020**, *385*, 123464. [[CrossRef](#)]
12. Wu, Q.; Xu, Y.; Yao, Z.; Liu, A.; Shi, G. Supercapacitors based on flexible graphene/polyaniline nanofiber composite films. *ACS Nano* **2010**, *4*, 1963–1970. [[CrossRef](#)] [[PubMed](#)]
13. Xavier, M.G.; Venancio, E.C.; Pereira, E.C.; Leite, F.L.; Leite, E.R.; MacDiarmid, A.G.; Mattoso, L.H.C. Synthesis of nanoparticles and nanofibers of polyaniline by potentiodynamic electrochemical polymerization. *J. Nanosci. Nanotechnol.* **2009**, *9*, 2169–2172. [[CrossRef](#)] [[PubMed](#)]
14. Jackowska, K.; Bieguński, A.T.; Tagowska, M. Hard template synthesis of conducting polymers: A route to achieve nanostructures. *J. Solid State Electrochem.* **2008**, *12*, 437–443. [[CrossRef](#)]
15. Anilkumar, P.; Jayakannan, M. Large-scale synthesis of polyaniline nanofibers based on renewable resource molecular template. *J. Appl. Polym. Sci.* **2009**, *4*, 3531–3541. [[CrossRef](#)]
16. Kimling, J.; Maier, M.; Okenve, B.; Kotaidis, V.; Ballot, H.; Plech, A. Turkevich method for gold nanoparticle synthesis revisited. *J. Phys. Chem. B* **2006**, *110*, 15700–15707. [[CrossRef](#)]
17. Stöber, W.; Fink, A.; Bohn, E. Controlled growth of monodisperse silica spheres in the micron size range. *J. Colloid Interface Sci.* **1968**, *26*, 62–69. [[CrossRef](#)]
18. Liu, J.; Qiao, S.Z.; Liu, H.; Chen, J.; Orpe, A.; Zhao, D.; Lu, G.Q. Extension of the stöber method to the preparation of monodisperse resorcinol-formaldehyde resin polymer and carbon spheres. *Angew. Chem. Int. Ed.* **2011**, *50*, 5947–5951. [[CrossRef](#)]
19. Iijima, S.; Ichihashi, T. Single-shell carbon nanotubes of 1-nm diameter. *Nature* **1993**, *363*, 603–605. [[CrossRef](#)]
20. Stankovich, S.; Dikin, D.A.; Piner, R.D.; Kohlhaas, K.A.; Kleinhammes, A.; Jia, Y.; Wu, Y.; Nguyen, S.T.; Ruoff, R.S. Synthesis of graphene-based nanosheets via chemical reduction of exfoliated graphite oxide. *Carbon* **2007**, *45*, 1558–1565. [[CrossRef](#)]
21. Lv, R.; Robinson, J.A.; Schaak, R.E.; Sun, D.; Sun, Y.; Mallouk, T.E.; Terrones, M. Transition metal dichalcogenides and beyond: Synthesis, properties, and applications of single- and few-layer nanosheets. *Acc. Chem. Res.* **2015**, *48*, 56–64. [[CrossRef](#)]
22. Huang, J. Syntheses and applications of conducting polymer polyaniline nanofibers. *Pure Appl. Chem.* **2006**, *78*, 15–27. [[CrossRef](#)]
23. Wu, Y.; Wang, J.; Ou, B.; Zhao, S.; Wang, Z. Some important issues of the commercial production of 1-D nano-PANI. *Polymers* **2019**, *11*, 681. [[CrossRef](#)]
24. Gospodinova, N.; Terlemezyan, L. Conducting polymers prepared by oxidative polymerization: Polyaniline. *Prog. Polym. Sci.* **1998**, *23*, 1443–1484. [[CrossRef](#)]
25. Sun, Y.; Xia, Y. Shape-controlled synthesis of gold and silver nanoparticles. *Science* **2002**, *298*, 2176–2179. [[CrossRef](#)] [[PubMed](#)]
26. Haruta, M. Size- and support-dependency in the catalysis of gold. *Catal. Today* **1997**, *36*, 153–166. [[CrossRef](#)]
27. Tiktopulo, E.I.; Uversky, V.N.; Lushchik, V.B.; Klenin, S.I.; Bychkova, V.E.; Ptitsyn, O.B. “Domain” Coil–Globule Transition in Homopolymers. *Macromolecules* **1995**, *28*, 7519–7524. [[CrossRef](#)]

28. Allinger, N.L.; Yan, L.; Chen, K. Molecular mechanics calculations (MM2 and MM3) on enamines and aniline derivative. *J. Comput. Chem.* **1994**, *15*, 1321–1330. [CrossRef]
29. Kolla, H.S.; Surwade, S.P.; Zhang, X.; MacDiarmid, A.G.; Manohar, S.K. Absolute molecular weight of polyaniline. *J. Am. Chem. Soc.* **2005**, *127*, 16770–16771. [CrossRef] [PubMed]
30. Hsu, C.-H.; Peacock, P.M.; Flippen, R.B.; Manohar, S.K.; MacDiarmid, A.G. The molecular weight of polyaniline by light scattering and gel permeation chromatography. *Synth. Met.* **1993**, *60*, 233–237. [CrossRef]
31. Stejskal, J.; Gilbert, R.G. Polyaniline. Preparation of a conducting polymer (IUPAC technical report). *Pure Appl. Chem.* **2002**, *74*, 857–867. [CrossRef]
32. Manohar, S.K.; Macdiarmid, A.G.; Epstein, A.J. Polyaniline: Pernigranile, an isolable intermediate in the conventional chemical synthesis of emeraldine. *Synth. Met.* **1991**, *41*, 711–714. [CrossRef]
33. Li, D.; Kaner, R.B. Shape and aggregation control of nanoparticles: Not shaken, not stirred. *J. Am. Chem. Soc.* **2006**, *128*, 968–975. [CrossRef]
34. Li, D.; Kaner, R.B. Processable stabilizer-free polyaniline nanofiber aqueous colloids. *ChemComm* **2005**, *26*, 3286–3288. [CrossRef]
35. Huang, J.; Kaner, R.B. The intrinsic nanofibrillar morphology of polyaniline. *ChemComm* **2006**, *4*, 367–376. [CrossRef]
36. Huang, J.; Kaner, R.B. Nanofiber formation in the chemical polymerization of aniline: A mechanistic study. *Angew. Chem. Int. Ed.* **2004**, *43*, 5817–5821. [CrossRef] [PubMed]
37. Li, D.; Kaner, R.B. How nucleation affects the aggregation of nanoparticles. *J. Mater. Chem. A* **2007**, *17*, 2279–2282. [CrossRef]
38. Tran, H.D.; Wang, Y.; D’Arcy, J.M.; Kaner, R.B. Toward an understanding of the formation of conducting polymer nanofibers. *ACS Nano* **2008**, *2*, 1841–1848. [CrossRef] [PubMed]
39. Mailhe-Randolph, C.; Desilvestro, J. Morphology of electropolymerized aniline films modified by para-phenylenediamine. *J. Electroanal. Chem.* **1989**, *262*, 289–295. [CrossRef]
40. Tran, H.D.; Kaner, R.B. A general synthetic route to nanofibers of polyaniline derivatives. *ChemComm* **2006**, *37*, 3915–3917. [CrossRef]
41. Li, X.-G.; Li, A.; Huang, M.-R. Facile High-Yield Synthesis of Polyaniline Nanosticks with Intrinsic Stability and Electrical Conductivity. *Chem. Eur. J.* **2008**, *14*, 10309–10317. [CrossRef]
42. Trchová, M.; Šeděnková, I.; Konyushenko, E.N.; Stejskal, J.; Holler, P. Evolution of polyaniline nanotubes: The oxidation of aniline in water. *J. Phys. Chem. B* **2006**, *110*, 9461–9468. [CrossRef]
43. Blinova, N.V.; Stejskal, J.; Trchová, M.; Prokeš, J. Polyaniline prepared in solutions of phosphoric acid: Powders, thin films, and colloidal dispersions. *Polymer* **2006**, *47*, 42–48. [CrossRef]
44. Riede, A.; Helmstedt, M.; Sapurina, I.; Stejskal, J. In situ polymerized polyaniline films: 4 Film formation in dispersion polymerization of aniline. *J. Colloid Interface Sci.* **2002**, *248*, 413–418. [CrossRef]
45. Stejskal, J.; Špírková, M.; Kratochvíl, P. Polyaniline dispersions 4. Polymerization seeded by polyaniline particles. *Acta Polym.* **1994**, *45*, 385–388. [CrossRef]
46. Sulimenko, T.; Stejskal, J.; Křivka, I.; Prokeš, J. Conductivity of colloidal polyaniline dispersions. *Eur. Polym. J.* **2001**, *37*, 219–226. [CrossRef]
47. Stejskal, J.; Sapurina, I.; Trchová, M. Polyaniline nanostructures and the role of aniline oligomers in their formation. *Prog. Polym. Sci.* **2010**, *35*, 1420–1481. [CrossRef]
48. Trchová, M.; Stejskal, J. Polyaniline: The infrared spectroscopy of conducting polymer nanotubes. *Pure Appl. Chem.* **2011**, *83*, 1803–1817. [CrossRef]
49. Stejskal, J.; Sapurina, I.; Trchová, M.; Konyushenko, E.N. Oxidation of aniline: Polyaniline granules, nanotubes, and oligoaniline microspheres. *Macromolecules* **2008**, *41*, 3530–3536. [CrossRef]
50. Luo, C.; Peng, H.; Zhang, L.; Lu, G.-L.; Wang, Y.; Travas-Sejdic, J. Formation of nano-/microstructures of polyaniline and its derivatives. *Macromolecules* **2011**, *44*, 6899–6907. [CrossRef]
51. Feng, J.; Jing, X.; Li, Y. Self-assembly of aniline oligomers and their induced polyaniline supra-molecular structures. *Chem. Pap.* **2013**, *67*, 891–908. [CrossRef]
52. Laslau, C.; Zujovic, Z.D.; Zhang, L.; Bowmaker, G.A.; Travas-Sejdic, J. Morphological evolution of self-assembled polyaniline nanostructures obtained by pH-stat chemical oxidation. *Chem. Mater.* **2009**, *21*, 954–962. [CrossRef]
53. Laslau, C.; Zujovic, Z.D.; Travas-Sejdic, J. Polyaniline “Nanotube” self-assembly: The stage of granular agglomeration on nanorod templates. *Macromol. Rapid Commun.* **2009**, *30*, 1663–1668. [CrossRef]
54. Venancio, E.C.; Wang, P.-C.; MacDiarmid, A.G. The azanes: A class of material incorporating nano/micro self-assembled hollow spheres obtained by aqueous oxidative polymerization of aniline. *Synth. Met.* **2006**, *156*, 357–369. [CrossRef]
55. Venancio, E.C.; Wang, P.-C.; Toledo, O.Y.; MacDiarmid, A.G. First preparation of optical quality films of nano/micro hollow spheres of polymers of aniline. *Synth. Met.* **2007**, *157*, 758–763. [CrossRef]
56. Willstätter, R.; Moore, C.W. Über Anilinschwarz. I. *Ber. Dtsch. Chem. Ges.* **1907**, *40*, 2665–2689. [CrossRef]
57. Green, A.G.; Woodhead, A.E. CCXLIII—Aniline-black and allied compounds. Part I. *J. Chem. Soc. Trans.* **1910**, *97*, 2388–2403. [CrossRef]
58. Available online: <https://pubchem.ncbi.nlm.nih.gov/compound/Aniline-Black> (accessed on 23 December 2022).
59. Li, Y.; Zheng, J.-L.; Feng, J.; Jing, X.-L. Polyaniline micro-/nanostructures: Morphology control and formation mechanism exploration. *Chem. Pap.* **2013**, *67*, 876–890. [CrossRef]

60. Wang, P.-C.; Venancio, E.C.; Sarno, D.M.; MacDiarmid, A.G. Simplifying the reaction system for the preparation of polyaniline nanofibers: Re-examination of template-free oxidative chemical polymerization of aniline in conventional low-pH acidic aqueous media. *React. Funct. Polym.* **2009**, *69*, 217–223. [\[CrossRef\]](#)
61. Zhang, X.; Kolla, H.S.; Wang, X.; Raja, K.; Manohar, S.K. Fibrillar growth in polyaniline. *Adv. Funct. Mater.* **2006**, *16*, 1145–1152. [\[CrossRef\]](#)
62. Neelgund, G.M.; Oki, A. A facile method for the synthesis of polyaniline nanospheres and the effect of doping on their electrical conductivity. *Polym. Int.* **2011**, *60*, 1291–1295. [\[CrossRef\]](#)
63. Yalkowsky, S.H.; He, Y.; Jain, P. *Handbook of Aqueous Solubility Data*, 2nd ed.; CRC Press: Boca Raton, FL, USA, 2010; p. 259.
64. Ayad, M.; El-Hefnawy, G.; Zaghlol, S. Facile synthesis of polyaniline nanoparticles; its adsorption behavior. *Chem. Eng. J.* **2013**, *217*, 460–465. [\[CrossRef\]](#)
65. Neira-Carrillo, A.; Yslas, E.; Marini, Y.A.; Vásquez-Quitral, P.; Sánchez, M.; Riveros, A.; Yáñez, D.; Cavallo, P.; Kogan, M.J.; Acevedo, D. Hybrid biomaterials based on calcium carbonate and polyaniline nanoparticles for application in photothermal therapy. *Colloids Surf. B* **2016**, *145*, 634–642. [\[CrossRef\]](#)
66. Li, G.; Zhang, C.; Peng, H. Facile synthesis of self-assembled polyaniline nanodisks. *Macromol. Rapid Commun.* **2008**, *29*, 63–67. [\[CrossRef\]](#)
67. Mahato, N.; Parveen, N.; Cho, M.H. Synthesis of highly crystalline polyaniline nanoparticles by simple chemical route. *Mater. Lett.* **2015**, *161*, 372–374. [\[CrossRef\]](#)
68. Wang, Y.; Jing, X. Formation of polyaniline nanofibers: A morphological study. *J. Phys. Chem. B* **2008**, *112*, 1157–1162. [\[CrossRef\]](#)
69. Amarnath, C.A.; Kim, J.; Kim, K.; Choi, J.; Sohn, D. Nanoflakes to nanorods and nanospheres transition of selenious acid doped polyaniline. *Polymer* **2008**, *49*, 432–437. [\[CrossRef\]](#)
70. Lin, M.; Wang, D.; Li, S.; Tang, Q.; Liu, S.; Ge, R.; Liu, Y.; Zhang, D.; Sun, H.; Zhang, H.; et al. Cu(II) doped polyaniline nanoshuttles for multimodal tumor diagnosis and therapy. *Biomaterials* **2016**, *104*, 213–222. [\[CrossRef\]](#)
71. Sapurina, I.; Shishov, M. Oxidative Polymerization of Aniline: Molecular Synthesis of Polyaniline and the Formation of Supramolecular Structures. In *New Polymers for Special Applications*; De Souza-Gomes, A., Ed.; IntechOpen: London, UK, 2012. [\[CrossRef\]](#)
72. Bi, S.; Li, M.; Liang, Z.; Li, G.; Yu, G.; Zhang, J.; Chen, C.; Yang, C.; Xue, C.; Zuo, Y.Y.; et al. Self-assembled aluminum oxyhydroxide nanorices with superior suspension stability for vaccine adjuvant. *J. Colloid Interface Sci.* **2022**, *627*, 238–246. [\[CrossRef\]](#)
73. German, N.; Popov, A.; Ramanaviciene, A.; Ramanavicius, A. Evaluation of enzymatic formation of polyaniline nanoparticles. *Polymer* **2017**, *115*, 211–216. [\[CrossRef\]](#)
74. Zeng, F.; Xiao, Y.; Shen, Y.; Xu, X.; Qin, Z. Facile template-free fabrication and charge storage behavior of polyaniline nanobelts by using the oxidation–reduction initiation system in various inorganic acids. *Electrochim. Acta* **2021**, *386*, 138516. [\[CrossRef\]](#)
75. Konyushenko, E.N.; Stejskal, J.; Šeděnková, I.; Trchová, M.; Sapurina, I.; Cieslar, M.; Prokeš, J. Polyaniline nanotubes: Conditions of formation. *Polym. Int.* **2006**, *55*, 31–39. [\[CrossRef\]](#)
76. Ran, F.; Tan, Y.-T.; Liu, J.; Zhao, L.; Kong, L.-B.; Luo, Y.-C.; Kang, L. Preparation of hierarchical polyaniline nanotubes based on self-assembly and its electrochemical capacitance. *Polym. Adv. Technol.* **2012**, *23*, 1297–1301. [\[CrossRef\]](#)
77. Sun, Q.; Park, M.-C.; Deng, Y. Studies on one-dimensional polyaniline (PANI) nanostructures and the morphological evolution. *Mater. Chem. Phys.* **2008**, *110*, 276–279. [\[CrossRef\]](#)
78. Hsieh, B.-Z.; Chuang, H.-Y.; Chao, L.; Li, Y.-J.; Huang, Y.-J.; Tseng, P.-H.; Hsieh, T.-H.; Ho, K.-S. Formation mechanism of a nanotubular polyanilines prepared by an emulsion polymerization without organic solvent. *Polymer* **2008**, *49*, 4218–4225. [\[CrossRef\]](#)
79. Haba, Y.; Segal, E.; Narkis, M.; Siegmann, A. Polymerization of aniline in the presence of DBSA in an aqueous dispersion. *Synth. Met.* **1999**, *106*, 59–66. [\[CrossRef\]](#)
80. do Nascimento, G.M.; Silva, C.H.B.; Izumi, C.M.S.; Temperini, M.L.A. The role of cross-linking structures to the formation of one-dimensional nano-organized polyaniline and their Raman fingerprint. *Spectrochim. Acta A Mol. Biomol. Spectrosc.* **2008**, *71*, 869–875. [\[CrossRef\]](#)
81. Zhang, Z.; Wei, Z.; Zhang, L.; Wan, M. Polyaniline nanotubes and their dendrites doped with different naphthalene sulfonic acids. *Acta Mater.* **2005**, *53*, 1373–1379. [\[CrossRef\]](#)
82. He, C.; Tan, Y.; Li, Y. Conducting polyaniline nanofiber networks prepared by the doping induction of camphor sulfonic acid. *J. Appl. Polym. Sci.* **2003**, *87*, 1537–1540. [\[CrossRef\]](#)
83. Shinde, S.D.; Jayakannan, M. Probing the molecular interactions at the conducting polyaniline nanomaterial surface via a pyrene fluorophore. *J. Phys. Chem. C* **2010**, *114*, 15491–15498. [\[CrossRef\]](#)
84. Janošević, A.; Ciric-Marjanovic, G.; Marjanović, B.; Trchová, M.; Stejskal, J. 3,5-Dinitrosalicylic acid-assisted synthesis of self-assembled polyaniline nanorods. *Mater. Lett.* **2010**, *64*, 2337–2340. [\[CrossRef\]](#)
85. Arenas, M.C.; Andablo, E.; Castaño, V.M. Synthesis of conducting polyaniline nanofibers from single and binary dopant agents. *J. Nanosci. Nanotechnol.* **2010**, *10*, 549–554. [\[CrossRef\]](#) [\[PubMed\]](#)
86. Ren, L.; Zhang, X.F. Preparation and characterization of polyaniline micro/nanotubes with dopant acid mordant dark yellow GG. *Synth. Met.* **2010**, *160*, 783–787. [\[CrossRef\]](#)
87. Zhang, L.; Peng, H.; Zujovic, Z.D.; Kilmartin, P.A.; Travas-Sejdic, J. Characterization of polyaniline nanotubes formed in the presence of amino acids. *Macromol. Chem. Phys.* **2007**, *208*, 1210–1217. [\[CrossRef\]](#)

88. Janošević, A.; Ćirić-Marjanović, G.; Marjanović, B.; Holler, P.; Trchová, M.; Stejskal, J. Synthesis and characterization of conducting polyaniline 5-sulfosalicylate nanotubes. *Nanotechnology* **2008**, *19*, 135606. [\[CrossRef\]](#)
89. Zhang, Z.; Wei, Z.; Wan, M. Nanostructures of polyaniline doped with inorganic acids. *Macromolecules* **2002**, *35*, 5937–5942. [\[CrossRef\]](#)
90. Ćirić-Marjanović, G.; Holclajtner-Antunović, I.; Mentus, S.; Bajuk-Bogdanović, D.; Ješić, D.; Manojlović, D.; Trifunović, S.; Stejskal, J. Self-assembled polyaniline 12-tungstophosphate micro/nanostructures. *Synth. Met.* **2010**, *160*, 1463–1473. [\[CrossRef\]](#)
91. Qiu, H.; Qi, S.; Wang, J.; Wang, D.; Wu, X. Synthesis of polyaniline nanorods using sucrose stearate as soft template. *Mater. Lett.* **2010**, *64*, 1964–1967. [\[CrossRef\]](#)
92. Qiu, H.; Qi, S.; Wang, D.; Wang, J.; Wu, X. Synthesis of polyaniline nanostructures via soft template of sucrose octaacetate. *Synth. Met.* **2010**, *160*, 1179–1183. [\[CrossRef\]](#)
93. Pahovnik, D.; Žagar, E.; Vohlidal, J.; Žigon, M. Effect of cations on polyaniline morphology. *Chem. Pap.* **2013**, *67*, 946–951. [\[CrossRef\]](#)
94. Li, X.; Zhao, Y.; Zhuang, T.; Wang, G.; Gu, Q. Self-dispersible conducting polyaniline nanofibres synthesized in the presence of β -cyclodextrin. *Colloids Surf. A Physicochem. Eng. Asp.* **2007**, *295*, 146–151. [\[CrossRef\]](#)
95. Li, X.; Zhuang, T.; Wang, G.; Zhao, Y. Stabilizer-free conducting polyaniline nanofiber aqueous colloids and their stability. *Mater. Lett.* **2008**, *62*, 1431–1434. [\[CrossRef\]](#)
96. Park, J.K.; Jeon, S.S.; Im, S.S. Effect of 4-sulfobenzoic acid monopotassium salt on oligoanilines for inducing polyaniline nanostructures. *Polymer* **2010**, *51*, 3023–3030. [\[CrossRef\]](#)
97. Li, W.; Wang, H.-L. Oligomer-Assisted Synthesis of Chiral Polyaniline Nanofibers. *J. Am. Chem. Soc.* **2004**, *126*, 2278–2279. [\[CrossRef\]](#)
98. Li, J.; Zhu, L.; Luo, W.; Liu, Y.; Tang, H. Correlation between one-directional helical growth of polyaniline and its optical activity. *J. Phys. Chem. C* **2007**, *111*, 8383–8388. [\[CrossRef\]](#)
99. Li, W.; Bailey, J.A.; Wang, H.-L. Toward optimizing synthesis of nanostructured chiral polyaniline. *Polymer* **2006**, *47*, 3112–3118. [\[CrossRef\]](#)
100. Yang, Y.; Wan, M. Chiral nanotubes of polyaniline synthesized by a template-free method. *J. Mater. Chem. A* **2002**, *12*, 897–901. [\[CrossRef\]](#)
101. Li, J.; Jia, Q.; Zhu, J.; Zheng, M. Interfacial polymerization of morphologically modified polyaniline: From hollow microspheres to nanowires. *Polym. Int.* **2008**, *57*, 337–341. [\[CrossRef\]](#)
102. Zhang, X.; Goux, W.J.; Manohar, S.K. Synthesis of Polyaniline Nanofibers by “Nanofiber Seeding”. *J. Am. Chem. Soc.* **2004**, *126*, 4502–4503. [\[CrossRef\]](#)
103. Xu, X.; Zhou, Y.; Shen, Y.; Yan, H.; Jin, D.; Qin, Z. Impact of isopropanol on nucleation and growth of polyaniline nanofibers towards capacitive charge storage enhancement. *Electrochim. Acta* **2021**, *398*, 139326. [\[CrossRef\]](#)
104. Morales, G.M. Estudio de la Sintesis y Propiedades de Poliarilaminas Modificadas. Ph.D. Thesis, Universidad Nacional de Río Cuarto, Río Cuarto, Argentina, 2002.
105. Morales, G.M.; Tuninetti, J.; Miras, M.C.; Barbero, C. Photolithography of polyaniline on solid substrates using photoassisted polymerization of aniline. *Mol. Cryst. Liq. Cryst.* **2010**, *522*, 89–96. [\[CrossRef\]](#)
106. Pillalamarri, S.K.; Blum, F.D.; Tokuhito, A.T.; Story, J.G.; Bertino, M.F. Radiolytic synthesis of polyaniline nanofibers: A new templateless pathway. *Chem. Mater.* **2005**, *17*, 227–229. [\[CrossRef\]](#)
107. Li, Z.-F.; Blum, F.D.; Bertino, M.F.; Kim, C.-S.; Pillalamarri, S.K. One-step fabrication of a polyaniline nanofiber vapor sensor. *Sens. Actuators B Chem.* **2008**, *134*, 31–35. [\[CrossRef\]](#)
108. Liu, S.; Wang, J.; Ou, J.; Zhou, J.; Chen, Y.; Yang, S. Fabrication of one dimensional polyaniline nanofibers by uv-assisted polymerization in the aqueous phase. *J. Nanosci. Nanotechnol.* **2010**, *10*, 933–940. [\[CrossRef\]](#)
109. Li, J.; Tang, H.; Zhang, A.; Shen, X.; Zhu, L. A new strategy for the synthesis of polyaniline nanostructures: From nanofibers to nanowires. *Macromol. Rapid Commun.* **2007**, *28*, 740–745. [\[CrossRef\]](#)
110. Jing, X.; Wang, Y.; Wu, D.; Qiang, J. Sonochemical synthesis of polyaniline nanofibers. *Ultrason. Sonochem.* **2007**, *14*, 75–80. [\[CrossRef\]](#) [\[PubMed\]](#)
111. Wang, J.; Zhang, K.; Zhao, L. Sono-assisted synthesis of nanostructured polyaniline for adsorption of aqueous Cr(VI): Effect of protonic acids. *Chem. Eng. J.* **2014**, *239*, 123–131. [\[CrossRef\]](#)
112. Ganesan, R.; Shanmugam, S.; Gedanken, A. Pulsed sonoelectrochemical synthesis of polyaniline nanoparticles and their capacitance properties. *Synth. Met.* **2008**, *158*, 848–853. [\[CrossRef\]](#)
113. Barbero, C.; Miras, M.C.; Kötz, R.; Haas, O. Comparative study of the ion exchange and electrochemical properties of sulfonated polyaniline (SPAN) and polyaniline (PANI). *Synth. Met.* **1993**, *55*, 1539–1544. [\[CrossRef\]](#)
114. Qiu, B.; Wang, J.; Li, Z.; Wang, X.; Li, X. Influence of acidity and oxidant concentration on the nanostructures and electrochemical performance of polyaniline during fast microwave-assisted chemical polymerization. *Polymers* **2020**, *12*, 310. [\[CrossRef\]](#)
115. Cooper, E.C.; Vincent, B. Electrically conducting organic films and beads based on conducting latex particles. *J. Phys. D* **1989**, *22*, 1580–1585. [\[CrossRef\]](#)
116. Stejskal, J.; Kratochvíl, P.; Koňák, C. Structural parameters of spherical particles prepared by dispersion polymerization of methyl methacrylate. *Polymer* **1991**, *32*, 2435–2442. [\[CrossRef\]](#)

117. Liu, J.; Yang, S.C. Novel colloidal polyaniline fibrils made by template guided chemical polymerization. *J. Chem. Soc. Chem. Commun.* **1991**, 1529–1531. [\[CrossRef\]](#)
118. Armes, S.P.; Aldissi, M. Novel colloidal dispersions of polyaniline. *J. Chem. Soc. Chem. Commun.* **1989**, 88–89. [\[CrossRef\]](#)
119. Dearmitt, C.; Armes, S.P. Synthesis of novel polyaniline colloids using chemically grafted poly(N-vinylpyrrolidone)-based stabilizers. *J. Colloid Interface Sci.* **1992**, *150*, 134–142. [\[CrossRef\]](#)
120. Armes, S.P.; Aldissi, M.; Agnew, S.; Gottesfeld, S. Aqueous Colloidal Dispersions of Polyaniline Formed by Using Poly(vinylpyridine)-Based Steric Stabilizers. *Langmuir* **1990**, *6*, 1745–1749. [\[CrossRef\]](#)
121. Idissi, M.; Armes, S.P. Colloidal dispersions of conducting polymers. *Prog. Org. Coat.* **1991**, *19*, 21–58. [\[CrossRef\]](#)
122. Armes, S.P.; Aldissi, M.; Hawley, M.; Beery, J.G.; Gottesfeld, S. Morphology and Structure of Conducting Polymers. *Langmuir* **1991**, *7*, 1447–1452. [\[CrossRef\]](#)
123. Bay, R.F.C.; Armes, S.P.; Pickett, C.J.; Ryder, K.S. Poly(1-vinylimidazole-co-4-aminostyrene): Steric stabilizer for polyaniline colloids. *Polymer* **1991**, *32*, 2456–2460. [\[CrossRef\]](#)
124. Vincent, B.; Waterson, J. Colloidal dispersions of electrically-conducting, spherical polyaniline particles. *J. Chem. Soc. Chem. Commun.* **1990**, *9*, 683–684. [\[CrossRef\]](#)
125. Stejskal, J.; Kratochvíl, P.; Gospodinova, N.; Terlemezyan, L.; Mokreva, P. Polyaniline dispersions: Preparation of spherical particles and their light-scattering characterization. *Polymer* **1992**, *33*, 4857–4858. [\[CrossRef\]](#)
126. Gospodinova, N.; Terlemezyan, L.; Mokreva, P.; Stejskal, J.; Kratochvíl, P. Preparation and characterization of aqueous polyaniline dispersions. *Eur. Polym. J.* **1993**, *29*, 1305–1309. [\[CrossRef\]](#)
127. Stejskal, J.; Kratochvíl, P.; Helmstedt, M. Polyaniline dispersions. 5. Poly(vinyl alcohol) and poly(N-vinylpyrrolidone) as steric stabilizers. *Langmuir* **1996**, *12*, 3389–3392. [\[CrossRef\]](#)
128. Banerjee, P.; Bhattacharyya, S.N.; Mandal, B.M. Poly(vinyl methyl ether) Stabilized Colloidal Polyaniline Dispersions. *Langmuir* **1995**, *11*, 2414–2418. [\[CrossRef\]](#)
129. Barisci, J.N.; Innis, P.C.; Kane-Maguire, L.A.P.; Norris, I.D.; Wallace, G.G. Preparation of chiral conducting polymer colloids. *Synth. Met.* **1997**, *84*, 181–182. [\[CrossRef\]](#)
130. Innis, P.C.; Norris, I.D.; Kane-Maguire, L.A.P.; Wallace, G.G. Electrochemical formation of chiral polyaniline colloids codoped with (+)- Or (–)-10-camphorsulfonic acid and polystyrene sulfonate. *Macromolecules* **1998**, *31*, 6521–6528. [\[CrossRef\]](#)
131. Gill, M.T.; Chapman, S.E.; DeArmitt, C.L.; Baines, F.L.; Dadswell, C.M.; Stamper, J.G.; Lawless, G.A.; Billingham, N.C.; Armes, S.P. A study of the kinetics of polymerization of aniline using proton NMR spectroscopy. *Synth. Met.* **1998**, *93*, 227–233. [\[CrossRef\]](#)
132. Stejskal, J.; Spirkova, M.; Riede, A.; Helmstedt, M.; Mokreva, P.; Prokes, J. Polyaniline dispersions 8. The control of particle morphology. *Polymer* **1999**, *40*, 2487–2492. [\[CrossRef\]](#)
133. Chin, B.D.; Park, O.O. Dispersion stability and electrorheological properties of polyaniline particle suspensions stabilized by poly(vinyl methyl ether). *J. Colloid Interface Sci.* **2001**, *234*, 344–350. [\[CrossRef\]](#)
134. Stejskal, J. Colloidal dispersions of conducting polymers. *J. Polym. Mater.* **2001**, *18*, 225–258.
135. Stejskal, J.; Sapurina, I. On the origin of colloidal particles in the dispersion polymerization of aniline. *J. Colloid Interface Sci.* **2004**, *274*, 489–495. [\[CrossRef\]](#)
136. Stejskal, J.; Sapurina, I. Polyaniline: Thin films and colloidal dispersions. *Pure Appl. Chem.* **2005**, *77*, 815–826. [\[CrossRef\]](#)
137. Blinova, N.V.; Sapurina, I.; Klimovič, J.; Stejskal, J. The chemical and colloidal stability of polyaniline dispersions. *Polym. Degrad. Stab.* **2005**, *88*, 428–434. [\[CrossRef\]](#)
138. Tosheva, L.; Gospodinova, N.; Vidal, L.; Mihai, I.; Defaux, M.; Ivanov, D.A.; Doyle, A.M. Monoparticulate films of polyaniline. *Thin Solid Film.* **2009**, *517*, 5459–5463. [\[CrossRef\]](#)
139. Chen, F.; Liu, P. Preparation of polyaniline/phosphorylated poly(vinyl alcohol) nanoparticles and their aqueous redispersion stability. *AIChE J.* **2011**, *57*, 599–605. [\[CrossRef\]](#)
140. Peřinka, N.; Držková, M.; Hajná, M.; Jašúrek, B.; Šulcová, P.; Srovný, T.; Kaplanová, M.; Stejskal, J. Thermal analysis of polyaniline poly(N-vinylpyrrolidone)-stabilized dispersions. *J. Therm. Anal. Calorim.* **2014**, *116*, 589–595. [\[CrossRef\]](#)
141. Zimmermann, C.A.; Ferreira, J.C., Jr.; Ramôa, S.D.A.D.S.; Barra, G.M.D.O. Facile approach to produce water-dispersible conducting polyaniline powder. *Synth. Met.* **2020**, *267*, 116451. [\[CrossRef\]](#)
142. Park, H.-W.; Kim, T.; Huh, J.; Kang, M.; Lee, J.E.; Yoon, H. Anisotropic growth control of polyaniline nanostructures and their morphology-dependent electrochemical characteristics. *ACS Nano* **2012**, *6*, 7624–7633. [\[CrossRef\]](#)
143. Anbalagan, A.C.; Sawant, S.N. Biopolymer stabilized water dispersible polyaniline for supercapacitor electrodes. *AIP Conf. Proc.* **2018**, *1942*, 140054. [\[CrossRef\]](#)
144. Anjali, M.K.; Bharath, G.; Rashmi, H.M.; Avinash, J.; Naresh, K.; Raju, P.N.; Raghu, H.V. Polyaniline-Pectin nanoparticles immobilized paper based colorimetric sensor for detection of Escherichia coli in milk and milk products. *Curr. Res. Food Sci.* **2022**, *5*, 823–834. [\[CrossRef\]](#)
145. Gonçalves, J.P.; de Oliveira, C.C.; da Silva Trindade, E.; Riegel-Vidotti, I.C.; Vidotti, M.; Simas, F.F. In vitro biocompatibility screening of a colloidal gum Arabic-polyaniline conducting nanocomposite. *Int. J. Biol. Macromol.* **2021**, *173*, 109–117. [\[CrossRef\]](#)
146. Cruz-Silva, R.; Arizmendi, L.; Del-Angel, M.; Romero-Garcia, J. pH- and thermosensitive polyaniline colloidal particles prepared by enzymatic polymerization. *Langmuir* **2007**, *23*, 8–12. [\[CrossRef\]](#) [\[PubMed\]](#)

147. Jasenská, D.; Kašpárková, V.; Vašíček, O.; Münster, L.; Minařík, A.; Káčerová, S.; Korábková, E.; Urbánková, L.; Vícha, J.; Capáková, Z.; et al. Enzyme-Catalyzed Polymerization Process: A Novel Approach to the Preparation of Polyaniline Colloidal Dispersions with an Immunomodulatory Effect. *Biomacromolecules* **2022**, *23*, 3359–3370. [[CrossRef](#)] [[PubMed](#)]
148. Abel, S.B.; Molina, M.A.; Rivarola, C.R.; Kogan, M.J.; Barbero, C.A. Smart polyaniline nanoparticles with thermal and photothermal sensitivity. *Nanotechnology* **2014**, *25*, 495602. [[CrossRef](#)] [[PubMed](#)]
149. Michaelson, J.C.; McEvoy, A.J. Interfacial polymerization of aniline. *J. Chem. Soc. Chem. Commun.* **1994**, 79–80. [[CrossRef](#)]
150. Huang, J.; Virji, S.; Weiller, B.H.; Kaner, R.B. Polyaniline nanofibers: Facile synthesis and chemical sensors. *J. Am. Chem. Soc.* **2003**, *125*, 314–315. [[CrossRef](#)]
151. Pramanik, S.; Karak, N.; Banerjee, S.; Kumar, A. Effects of solvent interactions on the structure and properties of prepared PANi nanofibers. *J. Appl. Polym. Sci.* **2012**, *126*, 830–836. [[CrossRef](#)]
152. Kamlet, M.J.; Abboud, J.-L.M.; Abraham, M.H.; Taft, R.W. Linear Solvation Energy Relationships. 23. A Comprehensive Collection of the Solvatochromic Parameters, π , α , and β , and Some Methods for Simplifying the Generalized Solvatochromic Equation. *J. Org. Chem.* **1983**, *48*, 2877–2887. [[CrossRef](#)]
153. Su, C.; Wang, G.; Huang, F.; Li, X. Effects of synthetic conditions on the structure and electrical properties of polyaniline nanofibers. *J. Mater. Sci.* **2008**, *43*, 197–202. [[CrossRef](#)]
154. Chen, C.-H.; Dai, Y.-F. Effect of chitosan on interfacial polymerization of aniline. *Carbohydr. Polym.* **2011**, *84*, 840–843. [[CrossRef](#)]
155. Nuraje, N.; Su, K.; Yang, N.-I.; Matsui, H. Liquid/liquid interfacial polymerization to grow single crystalline nanoneedles of various conducting polymers. *ACS Nano* **2008**, *2*, 502–506. [[CrossRef](#)]
156. Oueiny, C.; Berlioz, S.; Perrin, F.X. Assembly of polyaniline nanotubes by interfacial polymerization for corrosion protection. *Phys. Chem. Chem. Phys.* **2016**, *18*, 3504–3509. [[CrossRef](#)]
157. Zhang, X.; Chan-Yu-King, R.; Jose, A.; Manohar, S.K. Nanofibers of polyaniline synthesized by interfacial polymerization. *Synth. Met.* **2004**, *145*, 23–29. [[CrossRef](#)]
158. Li, W.; Zhang, Q.; Chen, D.; Li, L. Study on nanofibers of polyaniline via interfacial polymerization. *J. Macromol. Sci. A* **2006**, *43*, 1815–1824. [[CrossRef](#)]
159. Ding, S.; Mao, H.; Zhang, W. Fabrication of DBSA-doped polyaniline nanorods by interfacial polymerization. *J. Appl. Polym. Sci.* **2008**, *109*, 2842–2847. [[CrossRef](#)]
160. Xing, S.X.; Zheng, H.W.; Zhao, G.K. Preparation of Polyaniline Nanofibers via a Novel Interfacial Polymerization Method. *Synth. Met.* **2008**, *158*, 59–63. [[CrossRef](#)]
161. Kamarudin, S.; Rani, M.S.A.; Mohammad, M.; Mohammed, N.H.; Su'ait, M.S.; Ibrahim, M.A.; Asim, N.; Razali, H. Investigation on size and conductivity of polyaniline nanofiber synthesised by surfactant-free polymerization. *J. Mater. Res.* **2021**, *14*, 255–261. [[CrossRef](#)]
162. Sun, Q.; Deng, Y. The unique role of dl-tartaric acid in determining the morphology of polyaniline nanostructures during an interfacial oxidation polymerization. *Mater. Lett.* **2008**, *62*, 1831–1834. [[CrossRef](#)]
163. Dallas, P.; Stamopoulos, D.; Boukos, N.; Tzitzios, V.; Niarchos, D.; Petridis, D. Characterization, magnetic and transport properties of polyaniline synthesized through interfacial polymerization. *Polymer* **2007**, *48*, 3162–3169. [[CrossRef](#)]
164. Do Nascimento, G.M.; Kobata, P.Y.G.; Temperini, M.L.A. Structural and vibrational characterization of polyaniline nanofibers prepared from interfacial polymerization. *J. Phys. Chem. B* **2008**, *112*, 11551–11557. [[CrossRef](#)]
165. Morales, G.M.; Llusa, M.; Miras, M.C.; Barbero, C. Effects of high hydrochloric acid concentration on aniline chemical polymerization. *Polymer* **1997**, *38*, 5247–5250. [[CrossRef](#)]
166. Zeng, F.; Qin, Z.; Liang, B.; Li, T.; Liu, N.; Zhu, M. Polyaniline nanostructures tuning with oxidants in interfacial polymerization system. *Prog. Nat. Sci.* **2015**, *25*, 512–519. [[CrossRef](#)]
167. Cui, J.-F.; Bao, X.-M.; Sun, H.-X.; An, J.; Guo, J.-H.; Yang, B.-P.; Li, A. Preparation of superhydrophobic surfaces by cauliflower-like polyaniline. *J. Appl. Polym. Sci.* **2014**, *131*, 39767. [[CrossRef](#)]
168. Cassie, A.B.D.; Baxter, S. Wettability of porous surfaces. *Trans. Faraday Soc.* **1944**, *40*, 546–551. [[CrossRef](#)]
169. Manuel, J.; Ahn, J.-H.; Kim, D.-S.; Ahn, H.-J.; Kim, K.-W.; Kim, J.-K.; Jacobsson, P. Synthesis and electrochemical properties of polyaniline nanofibers by interfacial polymerization. *J. Nanosci. Nanotechnol.* **2012**, *12*, 3534–3537. [[CrossRef](#)]
170. Barbero, C.; Miras, M.C.; Schnyder, B.; Hass, O.; Kötz, R. Sulfonated polyaniline films as cation insertion electrodes for battery applications. Part 1.—Structural and electrochemical characterization. *J. Mater. Chem. B* **1994**, *4*, 1775–1783. [[CrossRef](#)]
171. Goel, S.; Gupta, A.; Singh, K.P.; Mehrotra, R.; Kandpal, H.C. Optical studies of polyaniline nanostructures. *Mater. Sci. Eng. A* **2007**, *443*, 71–76. [[CrossRef](#)]
172. Mu, S. Nanostructured polyaniline synthesized using interface polymerization and its redox activity in a wide pH range. *Synth. Met.* **2010**, *160*, 1931–1937. [[CrossRef](#)]
173. Jin, D.; Qin, Z.; Shen, Y.; Li, T.; Ding, L.; Chen, Y.; Zhang, Y. Enhancing the formation and capacitance properties of interfacial polymerized polyaniline nanofibers by introducing small alcohol molecules. *J. Solid State Electrochem.* **2018**, *22*, 1227–1236. [[CrossRef](#)]
174. Akbarinezhad, E.; Ebrahimi, M.; Sharif, F.; Faridi, H.R. Facile synthesis of polyaniline nanofibers in supercritical CO₂ with high yield. *Res. Chem. Intermed.* **2013**, *39*, 4137–4144. [[CrossRef](#)]
175. Gao, H.; Jiang, T.; Han, B.; Wang, Y.; Du, J.; Liu, Z.; Zhang, J. Aqueous/ionic liquid interfacial polymerization for preparing polyaniline nanoparticles. *Polymer* **2004**, *45*, 3017–3019. [[CrossRef](#)]

176. He, Y. One-dimensional polyaniline nanostructures synthesized by interfacial polymerization in a solids-stabilized emulsion. *Appl. Surf. Sci.* **2006**, *252*, 2115–2118. [\[CrossRef\]](#)
177. Bhadra, S.; Lee, J.H. Synthesis of higher soluble nanostructured polyaniline by vapor-phase polymerization and determination of its crystal structure. *J. Appl. Polym. Sci.* **2009**, *114*, 331–340. [\[CrossRef\]](#)
178. Yang, L.; Zhou, Y.; Xu, X.; Shen, Y.; Yan, H.; Qin, Z. Interior design of hierarchical micro/nanostructures for enhancing energy storage ability of polyanilines through frozen interfacial polymerization. *Electrochim. Acta* **2021**, *386*, 138448. [\[CrossRef\]](#)
179. Gao, N.; Yu, J.; Chen, S.; Xin, X.; Zang, L. Interfacial polymerization for controllable fabrication of nanostructured conducting polymers and their composites. *Synth. Met.* **2021**, *273*, 116693. [\[CrossRef\]](#)
180. Dallas, P.; Georgakilas, V. Interfacial polymerization of conductive polymers: Generation of polymeric nanostructures in a 2-D space. *Adv. Colloid Interface Sci.* **2015**, *224*, 46–61. [\[CrossRef\]](#)
181. Huang, J.; Moore, J.A.; Acquaye, J.H.; Kaner, R.B. Mechanochemical route to the conducting polymer polyaniline. *Macromolecules* **2005**, *38*, 317–321. [\[CrossRef\]](#)
182. Zhou, C.-F.; Du, X.-S.; Liu, Z.; Ringer, S.P.; Mai, Y.-W. Solid phase mechanochemical synthesis of polyaniline branched nanofibers. *Synth. Met.* **2009**, *159*, 1302–1307. [\[CrossRef\]](#)
183. Du, X.-S.; Zhou, C.-F.; Wang, G.-T.; Mai, Y.-W. Novel solid-state and template-free synthesis of branched polyaniline nanofibers. *Chem. Mater.* **2008**, *20*, 3806–3808. [\[CrossRef\]](#)
184. Bhadra, S.; Kim, N.H.; Rhee, K.Y.; Lee, J.H. Preparation of nanosize polyaniline by solid-state polymerization and determination of crystal structure. *Polym. Int.* **2009**, *58*, 1173–1180. [\[CrossRef\]](#)
185. Shao, W.; Jamal, R.; Xu, F.; Ubud, A.; Abdiryim, T. The effect of a small amount of water on the structure and electrochemical properties of solid-state synthesized polyaniline. *Materials* **2012**, *5*, 1811–1825. [\[CrossRef\]](#)
186. Bhandari, S.; Khastgir, D. Template-free solid state synthesis of ultra-long hairy polyaniline nanowire supercapacitor. *Mater. Lett.* **2014**, *135*, 202–205. [\[CrossRef\]](#)
187. Bhandari, S.; Khastgir, D. Synergistic effect of simultaneous dual doping in solvent-free mechanochemical synthesis of polyaniline supercapacitor comparable to the composites with multiwalled carbon nanotube. *Polymer* **2015**, *81*, 62–69. [\[CrossRef\]](#)
188. Barbero, C.A.; Acevedo, D.F. Mechanochemical Synthesis of Polyanilines and Their Nanocomposites: A Critical Review. *Polymers* **2023**, *15*, 133. [\[CrossRef\]](#)
189. Vauthier, C.; Bouchemal, K. Methods for the Preparation and Manufacture of Polymeric Nanoparticles. *Pharm. Res.* **2009**, *26*, 1025–1058. [\[CrossRef\]](#)
190. Stockton, W.B.; Rubner, M.F. Molecular-level processing of conjugated polymers. 4. Layer-by-layer manipulation of polyaniline via hydrogen-bonding interactions. *Macromolecules* **1997**, *30*, 2717–2725. [\[CrossRef\]](#)
191. Cheung, J.H.; Stockton, W.B.; Rubner, M.F. Molecular-level processing of conjugated polymers. 3. Layer-by-layer manipulation of polyaniline via electrostatic interactions. *Macromolecules* **1997**, *30*, 2712–2716. [\[CrossRef\]](#)
192. Abel, S.B.; Yslas, E.I.; Rivarola, C.R.; Barbero, C.A. Synthesis of polyaniline (PANI) and functionalized polyaniline (F-PANI) nanoparticles with controlled size by solvent displacement method. Application in fluorescence detection and bacteria killing by photothermal effect. *Nanotechnology* **2018**, *29*, 125604. [\[CrossRef\]](#)
193. Chia, M.-R.; Phang, S.-W.; Ahmad, I. Emerging Applications of Versatile Polyaniline-Based Polymers in the Food Industry. *Polymers* **2022**, *14*, 5168. [\[CrossRef\]](#)
194. Mostafa, M.H.; Ali, E.S.; Darwish, M.S.A. Polyaniline/carbon nanotube composites in sensor applications. *Mater. Chem. Phys.* **2022**, *291*, 126699. [\[CrossRef\]](#)
195. Osuna, V.; Vega-Rios, A.; Zaragoza-Contreras, E.A.; Estrada-Moreno, I.A.; Dominguez, R.B. Progress of Polyaniline Glucose Sensors for Diabetes Mellitus Management Utilizing Enzymatic and Non-Enzymatic Detection. *Biosensors* **2022**, *12*, 137. [\[CrossRef\]](#)
196. da Silva, B.N.; Vieira, M.F.; Izumi, C.M.S. In situ preparation of silver nanoparticles on polyaniline nanofibers for SERS applications. *Synth. Met.* **2022**, *291*, 117171. [\[CrossRef\]](#)
197. Popov, A.; Aukstakojyte, R.; Gaidukevic, J.; Lisyte, V.; Kausaite-Minkstiniene, A.; Barkauskas, J.; Ramanaviciene, A. Reduced graphene oxide and polyaniline nanofibers nanocomposite for the development of an amperometric glucose biosensor. *Sensors* **2021**, *21*, 948. [\[CrossRef\]](#)
198. Nate, Z.; Gill, A.A.S.; Chauhan, R.; Karpoomath, R. Polyaniline-cobalt oxide nanofibers for simultaneous electrochemical determination of antimalarial drugs: Primaquine and proguanil. *Microchem. J.* **2021**, *160*, 105709. [\[CrossRef\]](#)
199. Zou, Y.; Chen, Z.; Guo, X.; Peng, Z.; Yu, C.; Zhong, W. Mechanically Robust and Elastic Graphene/Aramid Nanofiber/Polyaniline Nanotube Aerogels for Pressure Sensors. *ACS Appl. Mater. Interfaces* **2022**, *14*, 17858–17868. [\[CrossRef\]](#) [\[PubMed\]](#)
200. Thakur, B.; Amarnath, C.A.; Mangoli, S.H.; Sawant, S.N. Polyaniline nanoparticle based colorimetric sensor for monitoring bacterial growth. *Sens. Actuators B Chem.* **2015**, *207*, 262–268. [\[CrossRef\]](#)
201. Zhao, M.; Wu, X.; Cai, C. Polyaniline Nanofibers: Synthesis, Characterization, and Application to Direct Electron Transfer of Glucose Oxidase. *J. Phys. Chem. C* **2009**, *113*, 4987–4996. [\[CrossRef\]](#)
202. Rajesh; Ahuja, T.; Kumar, D. Recent progress in the development of nano-structured conducting polymers/nanocomposites for sensor applications. *Sens. Actuators B Chem.* **2009**, *136*, 275–286. [\[CrossRef\]](#)
203. Xie, J.; Gu, P.; Zhang, Q. Nanostructured Conjugated Polymers: Toward High-Performance Organic Electrodes for Rechargeable Batteries. *ACS Energy Lett.* **2017**, *2*, 1985–1996. [\[CrossRef\]](#)

204. Liu, B.; Zhu, K.; Ye, K.; Yan, J.; Wang, G.; Cao, D. Hierarchical conducting polymer coated conjugated polyimide anode towards durable lithium-ion batteries. *J. Power Sources* **2022**, *552*, 232226. [\[CrossRef\]](#)
205. Kim, J.; Lee, J.; You, J.; Park, M.-S.; Al Hossain, M.S.; Yamauchi, Y.; Kim, J.H. Conductive polymers for next-generation energy storage systems: Recent progress and new functions. *Mater. Horiz.* **2016**, *3*, 517–535. [\[CrossRef\]](#)
206. Kim, B.C.; Kwon, J.S.; Ko, J.M.; Park, J.H.; Too, C.O.; Wallace, G.G. Preparation and enhanced stability of flexible supercapacitor prepared from Nafion/polyaniline nanofiber. *Synth. Met.* **2010**, *160*, 94–98. [\[CrossRef\]](#)
207. Gao, Y.; Ying, J.; Xu, X.; Cai, L. Nitrogen-enriched carbon nanofibers derived from polyaniline and their capacitive properties. *Appl. Sci.* **2018**, *8*, 1079. [\[CrossRef\]](#)
208. Udayan, A.P.M.; Sadak, O.; Gunasekaran, S. Metal-Organic Framework/Polyaniline Nanocomposites for Lightweight Energy Storage. *ACS Appl. Energy Mater.* **2020**, *3*, 12368–12377. [\[CrossRef\]](#)
209. Banerjee, J.; Dutta, K.; Kader, M.A.; Nayak, S.K. An overview on the recent developments in polyaniline-based supercapacitors. *Polym. Adv. Technol.* **2019**, *30*, 1902–1921. [\[CrossRef\]](#)
210. Liu, S.; Dong, Z.; Wang, X.-Z.; Fu, X.-Z.; Luo, J.-L. Different acid doped polyaniline waterborne epoxy coatings: Anticorrosion and passivation performance on 5083 Al alloy. *Prog. Org. Coat.* **2022**, *173*, 107182. [\[CrossRef\]](#)
211. Pugacheva, T.A.; Malkov, G.V.; Ilyin, A.A.; Indeikin, E.A.; Kurbatov, V.G. Core/Shell Pigments with Polyaniline Shell: Optical and Physical-Technical Properties. *Polymers* **2022**, *14*, 2005. [\[CrossRef\]](#)
212. Fuseini, M.; Zaghoul, M.M.Y.; Elkady, M.F.; El-Shazly, A.H. Evaluation of synthesized polyaniline nanofibres as corrosion protection film coating on copper substrate by electrophoretic deposition. *J. Mater. Sci.* **2022**, *57*, 6085–6101. [\[CrossRef\]](#)
213. Abel, S.B.; Olejnik, R.; Rivarola, C.R.; Slobodian, P.; Saha, P.; Acevedo, D.F.; Barbero, C.A. Resistive Sensors for Organic Vapors Based on Nanostructured and Chemically Modified Polyanilines. *IEEE Sens. J.* **2018**, *18*, 6510–6516. [\[CrossRef\]](#)
214. Crean, C.; Lahiff, E.; Gilmartin, N.; Diamond, D.; O’Kennedy, R. Polyaniline nanofibres as templates for the covalent immobilisation of biomolecules. *Synth. Met.* **2011**, *161*, 285–292. [\[CrossRef\]](#)
215. Yslas, E.I.; Ibarra, L.E.; Peralta, D.O.; Barbero, C.A.; Rivarola, V.A.; Bertuzzi, M.L. Polyaniline nanofibers: Acute toxicity and teratogenic effect on *Rhinella arenarum* embryos. *Chemosphere* **2012**, *87*, 1374–1380. [\[CrossRef\]](#) [\[PubMed\]](#)
216. Ibarra, L.E.; Yslas, E.I.; Molina, M.A.; Rivarola, C.R.; Romanini, S.; Barbero, C.A.; Rivarola, V.A.; Bertuzzi, M.L. Near-infrared mediated tumor destruction by photothermal effect of PANI-Np in vivo. *Laser Phys.* **2013**, *23*, 066004. [\[CrossRef\]](#)
217. Kašpárková, V.; Jasenská, D.; Capáková, Z.; Maráková, N.; Stejskal, J.; Bober, P.; Lehocký, M.; Humpolíček, P. Polyaniline colloids stabilized with bioactive polysaccharides: Non-cytotoxic antibacterial materials. *Carbohydr. Polym.* **2019**, *219*, 423–430. [\[CrossRef\]](#)
218. Molina, M.A.; Rivarola, C.R.; Miras, M.C.; Lescano, D.; Barbero, C.A. Nanocomposite synthesis by absorption of nanoparticles into macroporous hydrogels. Building a chemomechanical actuator driven by electromagnetic radiation. *Nanotechnology* **2011**, *22*, 245504. [\[CrossRef\]](#)
219. Ghosh, S.; Amariei, G.; Mosquera, M.E.G.; Rosal, R. Conjugated polymer nanostructures displaying highly photoactivated antimicrobial and antibiofilm functionalities. *J. Mater. Chem. B* **2021**, *9*, 4390–4399. [\[CrossRef\]](#)
220. Pang, Q.; Wu, K.; Jiang, Z.; Shi, Z.; Si, Z.; Wang, Q.; Cao, Y.; Hou, R.; Zhu, Y. A Polyaniline Nanoparticles Crosslinked Hydrogel with Excellent Photothermal Antibacterial and Mechanical Properties for Wound Dressing Macromolecular. *Bioscience* **2022**, *22*, 2100386. [\[CrossRef\]](#)
221. Molina, M.; Asadian-Birjand, M.; Balach, J.; Bergueiro, J.; Miceli, E.; Calderón, M. Stimuli-responsive nanogel composites and their application in nanomedicine. *Chem. Soc. Rev.* **2015**, *44*, 6161–6186. [\[CrossRef\]](#)
222. Araújo, P.L.B.; Araújo, E.S.; Santos, R.F.S.; Pacheco, A.P.L. Synthesis and morphological characterization of PMMA/polyaniline nanofiber composites. *Microelectron. J.* **2005**, *36*, 1055–1057. [\[CrossRef\]](#)
223. Ghaleghafi, E.; Rahmani, M.B. Exploring different routes for the synthesis of 2D MoS₂/1D PANI nanocomposites and investigating their electrical properties. *Phys. E Low Dimens. Syst. Nanostruct.* **2022**, *138*, 115128. [\[CrossRef\]](#)
224. Yarmohamadi-Vasel, M.; Modarresi-Alam, A.R.; Noroozifar, M.; Hadavi, M.S. An investigation into the photovoltaic activity of a new nanocomposite of (polyaniline nanofibers)/(titanium dioxide nanoparticles) with different architectures. *Synth. Met.* **2019**, *252*, 50–61. [\[CrossRef\]](#)
225. Luo, Z.; Feng, S.; Li, Y.; Xu, G.; Fang, G.; Wang, S.; Zhu, C.; Liu, C. Synthesis of Conductive Polyaniline Composites for Superior Electromagnetic Wave Absorption with Lightweight and Broad Bandwidth. *Adv. Eng. Mater.* **2023**, *25*, 2200976. [\[CrossRef\]](#)
226. Zhang, P.; Han, X.; Kang, L.; Qiang, R.; Liu, W.; Du, Y. Synthesis and characterization of polyaniline nanoparticles with enhanced microwave absorption. *RSC Adv.* **2013**, *3*, 12694–12701. [\[CrossRef\]](#)
227. Yang, X.; Fan, B.; Wang, X.; Tang, X.; Wang, J.; Tong, G.; Wang, X.; Tian, W. HCl induced structure evolution and dual-frequency broadband microwave absorption of PANI hierarchical microtubes. *J. Environ. Chem. Eng.* **2021**, *9*, 105672. [\[CrossRef\]](#)
228. Su, S.; Yu, J.; Liu, X.; Yu, J. Fe nanoparticles embedded in polyaniline-derived carbon fibers as broad bandwidth microwave absorbers for GHz electromagnetic wave. *Solid State Commun.* **2021**, *334–335*, 114400. [\[CrossRef\]](#)
229. Bayat, A.; Tati, A.; Ahmadipouya, S.; Haddadi, S.A.; Arjmand, M. Electrospun chitosan/polyvinyl alcohol nanocomposite holding polyaniline/silica hybrid nanostructures: An efficient adsorbent of dye from aqueous solutions. *J. Mol. Liq.* **2021**, *331*, 115734. [\[CrossRef\]](#)
230. Lyu, W.; Yu, M.; Li, J.; Feng, J.; Yan, W. Adsorption of anionic acid red G dye on polyaniline nanofibers synthesized by FeCl₃ oxidant: Unravelling the role of synthetic conditions. *Colloids Surf. A Physicochem. Eng. Asp.* **2022**, *647*, 129203. [\[CrossRef\]](#)
231. Huang, W.S.; MacDiarmid, A.G. Optical properties of polyaniline. *Polymer* **1993**, *34*, 1833–1845. [\[CrossRef\]](#)

232. Barbero, C.; Kötz, R.; Haas, O. Differential photothermal deflection spectroscopy (DPDS). A technique to study electrochromism of synthetic metals. *Synth. Met.* **1999**, *101*, 170. [\[CrossRef\]](#)
233. Riberi, K.; Bongiovanni Abel, S.; Martinez, M.V.; Molina, M.A.; Rivarola, C.R.; Acevedo, D.F.; Rivero, R.; Cuello, E.A.; Gramaglia, R.; Barbero, C.A. Smart Thermomechanochemical Composite Materials Driven by Different Forms of Electromagnetic Radiation. *J. Compos. Sci.* **2020**, *4*, 3. [\[CrossRef\]](#)
234. Abel, S.B.; Rivarola, C.R.; Barbero, C.A.; Molina, M. Electromagnetic radiation driving of volume changes in nanocomposites made of a thermosensitive hydrogel polymerized around conducting polymer nanoparticles. *RSC Adv.* **2020**, *10*, 9155–9164. [\[CrossRef\]](#)
235. Bongiovanni Abel, S.; Molina, M.; Rivarola, C.R.; Barbero, C.A. Pickering emulsions stabilized with PANI-NP. Study of the thermoresponsive behavior under heating and radiofrequency irradiation. *J. Appl. Polym. Sci.* **2021**, *138*, 50625. [\[CrossRef\]](#)
236. Dong, Y.; Geng, C.; Liu, C.; Gao, J.; Zhou, Q. Near-infrared light photothermally induced shape memory and self-healing effects of epoxy resin coating with polyaniline nanofibers. *Synth. Met.* **2020**, *266*, 116417. [\[CrossRef\]](#)
237. Datta, S.; Barua, R.; Das, J. A Review on Electro-Rheological Fluid (ER) and Its Various Technological Applications. In *Extremophilic Microbes and Metabolites-Diversity, Bioprospecting and Biotechnological Applications*; Afef, N., Ameer, C., Haitham, S., Hadda, I.O., Eds.; IntechOpen: London, UK, 2020. [\[CrossRef\]](#)
238. Quadrat, O.; Stejskal, J. Polyaniline in electrorheology. *J. Ind. Eng. Chem.* **2006**, *12*, 352–361.
239. Wang, Y. Preparation and application of polyaniline nanofibers: An overview. *Polym. Int.* **2018**, *67*, 650–669. [\[CrossRef\]](#)
240. Abel, S.B.; Frontera, E.; Acevedo, D.; Barbero, C.A. Functionalization of Conductive Polymers through Covalent Postmodification. *Polymers* **2023**, *15*, 205. [\[CrossRef\]](#)
241. Guo, Y.; Zhou, Y. Polyaniline nanofibers fabricated by electrochemical polymerization: A mechanistic study. *Eur. Polym. J.* **2007**, *43*, 2292–2297. [\[CrossRef\]](#)
242. Karami, Z.; Youssefi, M.; Raeissi, K.; Zhiani, M. Morphology control of polyaniline nanostructures on the surface of reduced graphene oxide/cotton fabric composite electrode for high-performance wearable supercapacitor application. *J. Mater. Sci.* **2022**, *57*, 16776–16794. [\[CrossRef\]](#)
243. Rodriguez, R.C.; Moncada, A.B.; Acevedo, D.F.; Planes, G.A.; Miras, M.C.; Barbero, C.A. Electroanalysis using modified hierarchical nanoporous carbon materials. *Faraday Discuss.* **2014**, *164*, 147–173. [\[CrossRef\]](#) [\[PubMed\]](#)
244. Chang, C.; Wang, Y.; Horiuchi, Y.; Do Kim, H.; Fang, Y.; Ohkita, H.; Wang, B. Obvious improvement of dispersion of multiwall carbon nanotubes in polymer matrix through careful interface design. *Polym. Adv. Technol.* **2022**, *33*, 3350–3358. [\[CrossRef\]](#)
245. Sheldon, R.A. Green solvents for sustainable organic synthesis: State of the art. *Green Chem.* **2005**, *7*, 267–278. [\[CrossRef\]](#)
246. Mir, A.; Kumar, A.; Riaz, U. A short review on the synthesis and advance applications of polyaniline hydrogels. *RSC Adv.* **2022**, *12*, 19122–19132. [\[CrossRef\]](#)
247. Li, M.; Xu, B.; Zheng, L.; Zhou, J.; Luo, Z.; Li, W.; Ma, W.; Mao, Q.; Xiang, H.; Zhu, M. Highly stable polyaniline array@ partially reduced graphene oxide hybrid fiber for high-performance flexible supercapacitors. *Carbon* **2023**, *203*, 455–461. [\[CrossRef\]](#)
248. Yadav, A.; Kumar, H.; Sharma, R.; Kumari, R.; Thakur, M. Quantum dot decorated polyaniline plastic as a multifunctional nanocomposite: Experimental and theoretical approach. *RSC Adv.* **2022**, *12*, 24063–24076. [\[CrossRef\]](#) [\[PubMed\]](#)
249. Tanweer, M.S.; Iqbal, Z.; Alam, M. Experimental Insights into Mesoporous Polyaniline-Based Nanocomposites for Anionic and Cationic Dye Removal. *Langmuir* **2022**, *38*, 8837–8853. [\[CrossRef\]](#) [\[PubMed\]](#)
250. Hou, M.; Gu, H.; Huang, J.; Guan, H.; Xing, S. Three-dimensional polyaniline/cerium oxide composite aerogel with enhanced microwave absorption properties. *Synth. Met.* **2023**, *293*, 117251. [\[CrossRef\]](#)
251. Sahiner, N.; Demirci, S. In situ preparation of polyaniline within neutral, anionic, and cationic superporous cryogel networks as conductive, semi-interpenetrating polymer network cryogel composite systems. *J. Appl. Polym. Sci.* **2016**, *133*. [\[CrossRef\]](#)
252. Martínez, M.V.; Bongiovanni Abel, S.; Rivero, R.; Miras, M.C.; Rivarola, C.R.; Barbero, C.A. Polymeric nanocomposites made of a conductive polymer and a thermosensitive hydrogel: Strong effect of the preparation procedure on the properties. *Polymer* **2015**, *78*, 94–103. [\[CrossRef\]](#)
253. Suganya, N.; Jaisankar, V.; Sivakumar, E.K.T. Conducting Polymeric Hydrogel Electrolyte Based on Carboxymethylcellulose and Polyacrylamide/Polyaniline for Supercapacitor Applications. *Int. J. Nanosci.* **2018**, *17*, 1760003. [\[CrossRef\]](#)
254. Kovtyukhova, N.I.; Martin, B.R.; Mbindyo, J.K.N.; Mallouk, T.E.; Cabassi, M.; Mayer, T.S. Layer-by-layer self-assembly strategy for template synthesis of nanoscale devices. *Mater. Sci. Eng. C* **2002**, *19*, 255–262. [\[CrossRef\]](#)
255. Michel, M.; Ettingshausen, F.; Scheiba, F.; Wolz, A.; Roth, C. Using layer-by-layer assembly of polyaniline fibers in the fast preparation of high performance fuel cell nanostructured membrane electrodes. *Phys. Chem. Chem. Phys.* **2008**, *10*, 3796–3801. [\[CrossRef\]](#) [\[PubMed\]](#)
256. Zhang, C.; Zhou, Z.; Wang, X.; Liu, J.; Sun, J.; Wang, L.; Ye, W.; Pan, C. A multifunctional coating with silk fibroin/chitosan quaternary ammonium salt/heparin sodium for AZ31B magnesium alloy. *Mater. Today Commun.* **2023**, *34*, 105070. [\[CrossRef\]](#)
257. Balach, J.; Bruno, M.M.; Cotella, N.G.; Acevedo, D.F.; Barbero, C.A. Electrostatic self-assembly of hierarchical porous carbon microparticles. *J. Power Sources* **2012**, *199*, 386–394. [\[CrossRef\]](#)
258. Didier, F.; Alastuey, P.; Tirado, M.; Odorico, M.; Deschanel, X.; Toquer, G. Solar absorbers based on electrophoretically deposited carbon nanotubes using pyrocatechol violet as a charging agent. *Thin Solid Film.* **2023**, *764*, 139614. [\[CrossRef\]](#)
259. Zhao, H.; Isozaki, K.; Taguchi, T.; Yang, S.; Miki, K. Laying down of gold nanorods monolayers on solid surfaces for surface enhanced Raman spectroscopy applications. *Phys. Chem. Chem. Phys.* **2021**, *23*, 26822–26828. [\[CrossRef\]](#) [\[PubMed\]](#)

260. Saberi, Z.; Naderi, N.; Meymian, M.-R.Z. Improved optical and electrical stability of ZnO nanorods via electrophoretic deposition of graphene thin film. *J. Mater. Sci. Mater. Electron.* **2022**, *33*, 13367–13375. [[CrossRef](#)]
261. Dan, L.I.; Huang, J.; Kaner, R.B. Polyaniline nanofibers: A unique polymer nanostructure for versatile applications. *Acc. Chem. Res.* **2009**, *42*, 135–145. [[CrossRef](#)]
262. Barbero, C.A.; Acevedo, D.F. Manufacturing Functional Polymer Surfaces by Direct Laser Interference Patterning (DLIP): A Polymer Science View. *Nanomanufacturing* **2022**, *2*, 229–264. [[CrossRef](#)]
263. Cavallo, P.; Coneo Rodriguez, R.; Broglia, M.; Acevedo, D.F.; Barbero, C.A. Simple fabrication of active electrodes using direct laser transference. *Electrochim. Acta* **2014**, *116*, 194–202. [[CrossRef](#)]
264. Kim, S.; Oh, S.M.; Kim, S.Y.; Park, J.D. Role of adsorbed polymers on nanoparticle dispersion in drying polymer nanocomposite films. *Polymers* **2021**, *13*, 2960. [[CrossRef](#)] [[PubMed](#)]
265. Yu, J.; Yuan, Z.; Wang, L.; Chen, S.; Wei, W.; Zhang, F. Multi-nanocomponent-assembled films with exceptional capacitance performance and electromagnetic interference shielding. *Mater. Chem. Front.* **2022**, *6*, 2201–2210. [[CrossRef](#)]
266. Borchert, K.B.L.; Carrasco, K.H.; Steinbach, C.; Reis, B.; Gerlach, N.; Mayer, M.; Schwarz, S.; Schwarz, D. Tuning the pore structure of templated mesoporous poly(melamine-co-formaldehyde) particles toward diclofenac removal. *J. Environ. Manag.* **2022**, *324*, 116221. [[CrossRef](#)]

Disclaimer/Publisher’s Note: The statements, opinions and data contained in all publications are solely those of the individual author(s) and contributor(s) and not of MDPI and/or the editor(s). MDPI and/or the editor(s) disclaim responsibility for any injury to people or property resulting from any ideas, methods, instructions or products referred to in the content.